Recurring bleaching events disrupt the spatial properties of coral reef benthic communities across scales

Ford, Helen; Gove, Jamison M. ; Healey, John; Davies, Andrew; Graham, Nicholas; Williams, Gareth J.

Remote Sensing in Ecology and Conservation

DOI:
10.1002/rse2.355

Published: 01/02/2024

Peer reviewed version

Recurring bleaching events disrupt the spatial properties of coral reef benthic communities across scales

Helen V. Ford[1], Jamison M. Gove[2], John R. Healey[3], Andrew J. Davies[4], Nicholas A. J. Graham[5] and Gareth J. Williams[1*]

[1]School of Ocean Sciences, Bangor University, Anglesey, LL59 5AB, UK

[2]Ecosystem Sciences Division, Pacific Islands Fisheries Science Center, National Oceanic and Atmospheric Administration, 1845 Wasp Blvd., Honolulu, HI 96818, USA

[3]School of Natural Sciences, Bangor University, Bangor, Gwynedd, LL57 2UW, UK

[4]Department of Biological Sciences, University of Rhode Island, Kingston, RI, USA

[5]Lancaster Environment Centre, Lancaster University, UK

[*]Email: g.j.williams@bangor.ac.uk

Abstract: Marine heatwaves are causing recurring coral bleaching events on tropical reefs that are driving ecosystem change. Yet little is known about how bleaching and subsequent coral mortality impacts the spatial properties of tropical seascapes, such as patterns of organism spatial clustering and heterogeneity across scales. Changes in these spatial properties can offer insight into ecosystem recovery potential following disturbance. Here we repeatedly quantified coral reef benthic spatial properties around the circumference of an uninhabited tropical island in the central Pacific over a 9-year period that included a minor and severe marine heatwave. Benthic communities showed increased biotic homogenisation following both minor and mass bleaching, becoming more taxonomically similar with a less diverse intra-island community composition. Hard coral cover, which was highly spatially clustered around the island prior to bleaching, became less spatially clustered following

minor bleaching and was indiscernible from a random distribution across all scales (100-2000 m) following mass bleaching. Interestingly, the reduced degree of hard coral cover spatial clustering was already evident by the onset of mass bleaching and before any dramatic wholesale loss in island-mean coral cover occurred. Reductions in hard coral spatial clustering may therefore offer an early indication of the ecosystem becoming degraded prior to mass coral mortality. In contrast, the spatial clustering of competitive fleshy macroalgae remained unchanged through both bleaching events, while crustose coralline algae and fleshy turf algae became more spatially clustered at larger scales (200-700 m) following mass bleaching. Overall, benthic community spatial patterning became less predictable following bleaching and was no longer reflective of gradients in long-term environmental drivers that typically structure these remote reefs. Our findings provide novel insights into how climate-driven marine heatwaves can impact the spatial properties of coral reef communities over multiple scales.

Keywords: autocorrelation, biotic homogenisation, coral bleaching, marine heatwave, seascape ecology, spatial clustering, spatial properties

Introduction

Disturbance can be a natural and beneficial ecosystem component, making resources such as light and space available for new recruits and enabling more species to coexist (Pickett and White, 1985). Yet, more frequent and intense disturbances can trigger abrupt system-wide changes (Hobbs and Huennneke, 1992; Burton, Jentsch and Walker, 2020). Widespread and persistent disturbance can promote the spatial expansion of “winners”, often broadly-adapted species that benefit from the resulting conditions, while “losers” can be lost from the area and native diversity reduced (McKinney and Lockwood, 1999). This can result

in biotic homogenisation, a decrease in overall taxonomic diversity of ecological communities over time (Olden *et al.*, 2004). Biotic homogenisation is documented across terrestrial and marine ecosystems, including forest plant communities following human land use change (Vellend *et al.*, 2007), and fish assemblages following severe habitat loss (Richardson *et al.*, 2018).

As the climate continues to change, ecosystem disturbance dynamics are also changing (Coumou and Rahmstorf, 2012; Cheal *et al.*, 2017), including more frequent and longer-lasting marine heat waves that cause widespread coral bleaching on tropical reefs (Hughes *et al.*, 2018a). These extreme ocean temperatures break down the relationship between endosymbiotic algae and their coral host, and can lead to reduced coral growth and mortality (Glynn, 1983; Brown, 1997). Significant coral cover reduction following disturbance can result in novel coral assemblages (Hughes *et al.*, 2018b) and dominance by non-reef-building benthic organisms such as fleshy macroalgae (Graham *et al.*, 2015). Evidence suggests that coral reefs could persist into the future, but with novel compositions and ecosystem functions (Williams and Graham, 2019) and more homogenous benthic and fish communities (Hughes *et al.*, 2007; Darling, McClanahan and Côté, 2013; Edmunds, 2014; Bento *et al.*, 2016).

Changes to coral reef benthic communities following bleaching are well documented at organismal to ecosystem scales. “Winners” and “losers” are driven by the biological characteristics of the coral hosts and their endosymbionts (Woesik *et al.*, 2011; Dilworth *et al.*, 2021) and gradients in numerous abiotic factors (Robinson, Wilson and Graham, 2019; Evans *et al.*, 2020), including background temperature regimes (Safaie *et al.*, 2018) and prior exposure to thermal stress (Ateweberhan and McClanahan, 2010). However, much less is known about how bleaching and subsequent coral mortality affects the spatial properties of tropical benthic communities across scales. We do know that the natural patterns of spatial

organisation of coral reef benthic communities are, in part, structured by long-term gradients in environmental drivers, including surface wave energy and upwelling (Williams *et al.*, 2013; Aston *et al.*, 2019; Ford *et al.*, 2021a). However on many reefs, local and global human impacts such as climate change-induced ocean warming, coastal development, nutrient runoff and overfishing are now the dominant drivers of ecosystem state (Williams *et al.*, 2019), making the influence of natural environmental factors hard to distinguish (Ford et al., 2020; Williams et al., 2015a).

Like many substrate-bound organisms including terrestrial plants (Plotkin *et al.*, 2000; Réjou-Méchain *et al.*, 2011), coral reef benthic communities are spatially heterogeneous. Their patterns of spatial organisation are often non-random across the seascape, with many individual benthic taxa showing evidence of spatial clustering at sub-metre to kilometre scales (Aston et al., 2019; Edwards et al., 2017; Ford et al., 2021a; Pedersen et al., 2019). Such heterogeneity is reputed to be an important driver of species diversity (Hautier *et al.*, 2017), through the provision of prey refuges (Brusven and Rose, 1981) and increased available niche space (Stein, Gerstner and Kreft, 2014). Quantifying and maintaining the natural spatial heterogeneity of an ecosystem is therefore often a target for conservation management (Wang *et al.*, 2021). Importantly, disturbance events can temporarily disrupt patterns of biological clustering in natural ecosystems. For example, following severe wind disturbance, the degree of spatial clustering of trees in eastern North American forests was significantly increased at small scales (5-10 m), while clustering significantly decreased at larger scales (30-50 m) (Peterson, 2020). On tropical reefs, models suggest the degree of hard coral spatial clustering influences how they interact with neighbouring and competing benthic organisms, which in turn affects coral growth trajectories and ecosystem recovery potential following acute disturbance (Brito-Millán *et al.*, 2019).

Here we quantified changes in the spatial properties of coral reef benthic taxa across scales over a 9-year period that included two marine heatwaves that resulted in bleaching and subsequent coral mortality. Our study system was Jarvis Island, an uninhabited tropical oceanic island and one of the world's most remote coral reef ecosystems. Our data were collected through towed-diver digital image surveys (Kenyon *et al.*, 2006), yielding semi-continuous data across km-extents while preserving a high thematic resolution of the benthic communities (Ford *et al.*, 2021a). These data allowed us to ask whether and how the spatial properties of coral reef benthic communities are impacted by coral bleaching across scales in the absence of confounding local human impacts. Specifically, we asked: (i) did benthic community composition and homogeneity change following bleaching? (ii) did the levels of spatial clustering of individual benthic organisms change across scales following bleaching? (iii) are the intra-island spatial patterns of coral reef benthic communities still reflective of the environmental factors that normally structure these remote reefs following bleaching?

Materials and Methods

Study site and disturbance history

Jarvis Island (0°22′S, 160°01′W) is a U.S-affiliated tropical island in the Line Islands Archipelago and forms part of the Pacific Islands Marine National Monument (Fig. 1). Jarvis has lacked a permanent human population throughout its geological history and is one of the most remote coral reef islands in the world. Previously labelled by the Ocean Health Index as the "healthiest" coral reef in the world (Halpern *et al.*, 2012), Jarvis provides an opportunity to study the spatial ecology of coral reefs in the absence of confounding local human impacts (Ford et al., 2020; Williams et al., 2015a). Jarvis faces few threats aside from temperature stress; it has overall low coral disease prevalence (Brainard, Acoba and Asher, 2019), low frequencies of extreme wave events caused by tropical storms (Gove *et al.*, 2013), and a low

abundance of coral predators such as the crown-of-thorns starfish (*Acanthaster planci*) (Brainard, Acoba and Asher, 2019).

From late 2009 to early 2010, an El-Niño triggered ocean warming across the region (Williams *et al.*, 2010a; Vargas-Ángel *et al.*, 2011) that resulted in minor coral bleaching prevalence (~3%) at Jarvis (Barkley *et al.*, 2018). According to the National Oceanographic and Atmospheric Administration's (NOAA) Coral Reef Watch data, this period reached a maximum of 11.7 Degree Heating Weeks (NOAA Coral Reef Watch, 2000). Degree Heating Week (DHW) is a common measure to indicate the accumulated thermal stress experienced by coral reefs, and this value exceeded the 8 DHW threshold expected to cause severe and widespread coral bleaching (Skirving *et al.*, 2020). Jarvis then endured a second and more severe El-Niño triggered bleaching event that started in May 2015 and ended by May 2016, resulting in a 98% decline in mean live hard coral cover (Barkley *et al.*, 2018; Brainard *et al.*, 2018; Vargas-Ángel *et al.*, 2019). NOAA's Coral Watch data showed temperature stress at a maximum of 29.1 DHW (NOAA Coral Reef Watch, 2000).

Benthic community digital surveys and spatial processing

Digital benthic images were taken around the circumference (~13 km) of Jarvis' fore-reef habitat (reef slope facing the open ocean) by towed-divers between 2001 and 2017 as part of NOAA's Pacific Reef Assessment and Monitoring Programme (RAMP) surveys (Kenyon *et al.*, 2006). The diver, towed at ~ 3 km h^{-1} along a targeted depth contour of 15 m, attempted to maintain a height of ~1 m above the seafloor and captured images of the benthos at ~15 m intervals using a downward-facing SLR camera (Canon EOS 10-D/50-D) fitted with strobes. At this height, each image captured a mean area of 1.09 m^2 (Kenyon et al. 2006). The tow-board was fitted with a sub-surface temperature logger (SeaBird™ Electronics 39

subsurface pressure, temperature-depth recorder; 10 s sample rate, 0.002 °C accuracy), and a GPS on the boat (combined with a layback algorithm) georeferenced each image.

From the available Pacific RAMP surveys, we post-processed images from 2008, 2010, 2015 and 2017 as they (i) provided the best spatial coverage around the island (each year had at least 70% coastline coverage with adequate digital image replication, *see methods below*), (ii) provided time points before and after minor and severe coral bleaching, and (iii) included a 'baseline' survey year (2008) that represented ~10 years since any previous mass bleaching events, allowing substantial time for benthic community recovery to a pre-disturbance state in the absence of local human impacts (Sheppard, Harris and Sheppard, 2008; Gilmour *et al.*, 2013). The 2010 surveys occurred in April towards the end of the minor bleaching event. The surveys in 2015 also occurred in April, during the onset of mass coral bleaching but prior to any mass coral mortality (exact survey dates are detailed in Supplementary Table A1). The 2017 survey provided a snapshot of benthic condition 11 months after the mass bleaching event in 2015-2016.

Although the benthic surveys targeted 15 m depth, some differences in depth did occur. We controlled for large differences in depth by selecting images within a 8-20 m depth range and every alternate benthic image was also selected to ensure continuity with previous work (Ford *et al.*, 2021a). We used the analysis software CoralNet (Beijbom *et al.*, 2015) to overlay 10 stratified random points over the entirety of each image. The benthos under each point was then identified by a single analyst to ensure taxonomic consistency. Each hard coral, soft coral and macroalga was identified to genus where possible, resulting in a total of 30 benthic groupings across all images (Supplemental Table A2). These were later combined into eight higher-level benthic groups (hard coral, crustose coralline algae (CCA), calcifying macroalgae, soft coral, fleshy macroalgae, turf algae, other invertebrates and sand) (see Supplemental Table A3 for group descriptions). Using ArcGIS and a custom Python script

(Aston *et al.*, 2019), we created 100-m wide grid cells around Jarvis' fore-reef and spatially joined them to the image-derived benthic cover data. Where grid cells contained data from less than four images, we returned to the 'every alternate image' step in our workflow and, where possible, added additional data derived from images within the same grid cell. Following this, only grid cells containing at least four images in each of the survey years (70.5% of grid cells) were used in subsequent analyses (Ford *et al.*, 2021a).

Quantifying benthic community change and heterogeneity over time

We tested for an effect of survey year (fixed factor, 4 levels) on benthic community structure, defined as the relative percentage cover of benthic organisms (n=30, Supplemental Table A2), using a permutational analysis of variance (PERMANOVA) (Anderson, 2001) with the *adonis* function within the *vegan* package (Oksanen *et al.*, 2019) for R version 4.0.2 (R Core Team, 2020). We used island grid cells as replicates and analyses were based on square-root transformed data (to down-weight highly dominant benthic organisms), a Bray-Curtis similarity matrix, 999 permutations of the raw data, and type III (partial) sums-of-squares. Where the global model was significant, we used the function *adonis.pair* within the *EcolUtils* package (Salazar, 2020) to identify differences between years.

To assess for changes in benthic community heterogeneity over time, we used multivariate dispersion (Anderson, 2006). Multivariate dispersion is a measure of group variance, here representing the relative variation in the cover of benthic genera (where possible) across island grid cells (individual replicates) within each survey year (group). We formally tested for differences in the mean distance to centroid for each group using a Permutational Analysis of Multivariate Dispersions (PERMDISP) (Anderson, Ellingsen and McArdle, 2006) with the *vegan* functions *betadisper* and *permutest*. Relative changes in benthic communities over the four years were visualised using non-metric multidimensional

scaling (nMDS). To identify those benthic organisms most responsible for driving differences in community structure across years, we overlaid the correlations of the original benthic organisms with the ordination axes as a bi-plot using *envfit* (vectors scaled by square root of the r^2).

While each island grid cell contained benthic data from at least 4 images, the maximum number of images per grid cell differed within and between survey years. We therefore conducted a sensitivity analysis to assess what effect this might have on our benthic community analyses. For those grid cells containing more than four images, we randomly removed all but four of them and re-calculated the percentage cover of each benthic organism within each grid cell and repeated the above community analyses. The global effect of 'year' remained the same, regardless of the maximum number of images or permutation of four images, and we found no substantial changes in the relative patterns of biotic homogeneity (see Supplemental Table A4) or relative community dissimilarity between survey years (see Supplemental Fig. A1 for a more detailed description of the results from our sensitivity analysis). As a result, and to maximise the accuracy of the percentage cover estimates within any given grid cell, we did not constrain the upper limit of images within each grid cell during any of our subsequent analyses.

Quantifying benthic community spatial properties over time

We used the Moran's I statistic (Moran, 1950) to quantify the degree of spatial clustering across scales of the most abundant higher-level benthic groups (hard coral, turf algae, CCA and fleshy macroalgae; Supplemental Table A5-A8) using their percentage cover values over time. We did this in both directions around the island using a custom R function (Aston *et al.*, 2019; Ford *et al.*, 2021a). We defined the observed Moran's I value (OMI) as:

$$I = \frac{n}{S_0} \frac{\sum_{i=1}^{n} \sum_{j=1}^{n} w_{i,j}(x_i - \bar{x})(x_j - \bar{x})}{\sum_{i=1}^{n}(x_i - \bar{x})^2}$$

where n is the number of observations, $w_{i,j}$ is the matrix of weights according to the inverse Euclidean distance between observations, x_i is the observed value at location i, x_j is the observed value at location j, $\bar{x}$ is the mean value and S_0 is the sum of spatial weights. The spatial weights are defined as the inverse of the minimum distance, $d_{i,j}$, around the circumference of the island between locations i and j, as:

$$d_{i,j} = min\big((j-i),(n+i-j)\big)$$

$$w_{i,j} = \frac{1}{d_{i,j}}\ for\ i \neq j, 0\ otherwise$$

OMI values were calculated at the grid cell spatial resolution (100 m wide) and then again in a moving-window averaging process at increasing 100-m increments to a maximum of 2 km (limited by replication beyond that scale due to island size) (Aston *et al.*, 2019). At each scale we re-computed the Moran's I statistic and p-value for all possible 100 m grid cell starting locations of the moving window averaging process. This was iterated in both directions around the circumference of the island since spatial patterns in nature can be anisotropic. We report the range in OMI values for each scale from this process (shaded region in Fig. 4a and Fig. 5) and the scale at which the upper bound of p exceeded 0.05 (i.e. did not significantly differ from a random spatial distribution). Significant OMI values away from zero indicated that the spatial pattern of the variable in question at that scale was highly organised in space. Significant positive OMI values indicated spatial clustering (positive autocorrelation). OMI values became negative (over-dispersed) at larger scales, however none of these values significantly differed from a random distribution for any of our higher-level benthic groups (indicated by the dashed horizontal lines in Fig. 4a and Fig. 5) and were therefore not interpreted.

Quantifying environmental drivers

We quantified sub-surface seawater temperature and surface wave power at the grid cell resolution (100 m) to predict spatial variations in the cover of higher-level benthic groups over time. Previous work has shown these physical drivers to be spatially variable (Gove, Merrifield and Brainard, 2006) and important in structuring Jarvis' benthic communities across scales (Aston *et al.*, 2019; Ford *et al.*, 2021a). For example, sub-surface temperature gradients around Jarvis are a proxy for upwelling and seawater nutrient availability that positively correlate with hard coral cover (Aston *et al.*, 2019). Furthermore, the upper spatial scales at which higher-level benthic groups show evidence of spatial clustering around Jarvis correlate with the upper scales at which surface wave power is spatially clustered (Ford *et al.*, 2021a). We calculated mean sub-surface temperature per grid cell using data from the tow-board temperature-depth recorders collected during that survey year, as well as the two prior survey years closest in the timeseries with adequate spatial coverage (to capture longer-term spatial patterning in temperature gradients) (see Supplemental Fig. A2). Despite these temperature data representing a temporal snapshot, they capture the longer-term intra-island gradients in sub-surface temperature around Jarvis (Aston et al. 2019, see Supplemental Fig. A2). Furthermore, these data allowed for estimates of spatially explicit sub-surface temperature variation within each 100-m grid cell. The limited number (n=5) of permanently deployed seabed-mounted temperature loggers around Jarvis within our study depth range lacked this spatial resolution (Aston et al. 2019).

To calculate surface wave power, data were extracted from NOAA's Wave Watch III 50-km resolution global model (http://polar.ncep.noaa.gov/waves). From the centre point of each 100-m grid cell, we created a 360° plot of lines (each line set to 100 km length) at 1° bearing intervals and used a vectorised shoreline of Jarvis and the surrounding islands to identify where each line intersected land, either on the island itself or a neighbouring island.

Where this occurred, that degree bin was removed, leaving only bearings open to exposure along the incident wave swath. For each of these exposed degree bins, wave power and its corresponding direction were selected at each time-step for the closest Wave Watch III pixel to the centroid of Jarvis; only waves that travelled along an open bearing were retained. Wave power (*WP* in W m^{-1}) was calculated from significant wave height (H_s) and peak period (T_p), which we extracted from Wave Watch III and defined as:

$$WP = \frac{\rho g^2 T_p H^2{}_s}{64\pi}$$

where ρ is the density of seawater (1024 kg m^{-3}) and g is the acceleration of gravity (9.8 m s^{-2}). For high energy wave events, a key driver of benthic community structure (Gove *et al.*, 2015), we calculated the mean of 9 maximum daily wave power values for each survey year and the prior three years closest in the timeseries for each grid cell. We averaged across these four years to reflect the long-term spatial patterning in these anomalies around Jarvis for each survey year (see Supplemental Fig. A2).

Quantifying the predictability of benthic communities following bleaching

To assess for changes in the ability to predict benthic community patterns from gradients in environmental drivers following bleaching, we modelled changes in crustose coralline algae (CCA) and turf algae cover. These benthic organisms were modelled (and not hard coral or fleshy macroalgae) due to their high abundance across the island in all survey years. This ensured that any changes in their predictability were a result of their driver-response relationship breaking down, rather than a loss of spatial replication leading to poor model performance. Here we focused on the changes in benthic organism spatial predictability over time rather than the nature and directionality of the bio-physical

relationships themselves, which have been extensively quantified for Jarvis in previous work (Aston *et al.*, 2019).

We used boosted regression trees (BRTs) (Breiman *et al.*, 1984; Elith, Leathwick and Hastie, 2008) to model the relationships between gradients in CCA and turf algae cover and our two environmental drivers, building a separate model for each survey year. We also added a categorical predictor corresponding to the NOAA-defined geo-regions around Jarvis (Brainard *et al.*, 2019) to account for any influence of other biophysical variables that we did not measure (see Supplemental Fig. A2). BRTs are a non-linear regression technique that combine large numbers of simple regression trees by sequentially fitting each new tree to the residuals from the previous one to improve overall predictive performance (Buston and Elith, 2011). Prior to model building, we assessed the collinearity in our continuous predictors using Pearson's correlation coefficient (*r*). Since *r* ranged from 0.31 to 0.06 across the survey years, both environmental drivers were included in all models (Dormann *et al.*, 2013). BRTs were constructed using the package *gbm* (Rigdeway, 2015) using a Gaussian distribution for the response variables.

BRT model performance was quantified using l0-fold cross validation. This involved splitting the data into 10 training sets (nine unique subsets of the data used for training, one omitted and used for testing) (Elith, Leathwick and Hastie, 2008). A BRT model is built on each training set and in each case model performance is tested with the remaining omitted data (Elith, Leathwick and Hastie, 2008). Mean model performance is reported as the cross-validated percentage deviance explained (1 – (cross-validated deviance/mean total deviance)) and was calculated using the R package *ggBRT* (Jouffray *et al.*, 2019). We optimised model performance by running combinations of the tree complexity (1,2,3,4,5), learning rate (0.001, 0.0001, 0.00001) and bag fraction (0.1, 0.5, 0.75) parameters, and identified the combination

that resulted in the lowest cross-validation deviance (CVD) for each individual BRT model (Williams *et al.*, 2010b) (see Supplemental Table A9 for optimal settings used).

To further explore changes in the ability to predict benthic community patterns from gradients in environmental drivers following bleaching, we also modelled the relationships between the percentage cover of all 30 benthic variables, sub-surface seawater temperature and surface wave power using permutational distance-based multivariate multiple regression (McArdle and Anderson, 2001). Models were constructed using square-root transformed benthic cover data and a Bray-Curtis similarity matrix using the PERMANOVA+ add-on (Anderson, Gorley and Clarke, 2008) for PRIMER v.7 (Clarke and Gorley, 2015). The environmental predictors were normalised to account for their variations in units and ranges. All possible candidate models (unique combinations of the predictors) were computed, and we report the percentage variation in the response variable explained by the top candidate model for each survey year.

Results

Changes in benthic community structure and heterogeneity over time

The relative cover of benthic organisms changed following both minor and mass bleaching (Fig. 2a). Island-mean hard coral cover (all hard coral genera combined) declined from 29.2% in 2008 (± 2.8 SE) to 22.8% (± 2.2) in 2010 following minor bleaching. During the reprieve from disturbance between 2010 and 2015, island-mean hard coral cover increased to 27.0% (± 1.5) (Fig. 2a). During this entire period, hard coral communities were dominated by *Montipora* and *Pocillopora* (Fig. 2b, Supplemental Table A5-A7). CCA were also very abundant with an island-mean cover of 33.8% in 2008 that increased to 50.5% in 2010 following minor bleaching. Following mass bleaching, island-mean hard coral cover dropped to just 0.3% (± 0.1) by 2017, while there was a notable increase in turf algae and

fleshy macroalgae (Fig. 2a). CCA also continued to dominate much of the seascape in 2017 (39.6%) following mass bleaching (Fig. 2a). Following mass bleaching there was a marked change in genera dominating the coral communities. The previously dominant *Montipora* gave way to *Pocillopora* and *Porites* and to a lesser extent *Favites*, *Favia and Turbinaria* dominating the surviving communities (Fig. 2b, Supplemental Table A5-A8).

Benthic community structure changed significantly over time following the two bleaching events (Pseudo-$F_{3,335}$= 49.5, p=0.001, Fig. 3a), with communities significantly different following minor bleaching (2008 vs 2010, p=<0.001) and following mass bleaching (p=<0.001 for both 2008 vs 2017 and 2015 vs 2017). Prior to the bleaching events, the benthos was characterised by a higher cover of the hard corals *Montipora, Pocillopora* and *Acropora* and the soft coral *Sinularia*, than in the subsequent years (Fig. 3b). Following minor bleaching in 2010 and by the onset of mass bleaching in 2015, benthic communities were characterised by CCA and the fleshy macroalga *Lobophora,* the hard coral *Favites* and the fire coral *Millepora*. Benthic communities were markedly different again following mass bleaching (Fig. 3a) and were characterised by a higher cover of turf algae, the fleshy macroalga *Galaxuara*, *Dictyosphaeria* and *Lobophora*, cyanobacteria, and the encrusting calcified macroalga *Peyssonelia* (Fig. 3b).

Benthic communities also displayed increased homogeneity (had lower multivariate dispersion) over time (Fig. 3a). Multivariate dispersion was significantly lower following minor bleaching (2008 vs 2010, p=0.024) and then remained stable during the onset of mass bleaching (2010 vs 2015, p=0.883). The communities then became more homogenous again following mass bleaching (2015 vs 2017, p=0.044). Overall, the multivariate dispersion was significantly lower following the two bleaching events than at the start of the timeseries (2008 vs 2017, p=0.001). This pattern held when standardising the number of benthic images per grid cell (by limiting to four) around the island (see Supplemental Table A4).

Changes in benthic community spatial properties over time

Hard coral cover displayed similar patterns of spatial structure in 2008 and following minor bleaching in 2010, with cover significantly clustered up to 1.2 and 1.1 km scales, respectively (Fig. 4a). By the onset of mass bleaching in 2015, hard coral cover was only significantly clustered up to 0.5 km scales and the degree of clustering (mean OMI value) had almost halved (Fig. 4a). This appeared to be driven by a reduction in cover along the island's west coast, and localised increases in other locations, resulting in a more even distribution of coral cover around the island compared with earlier years (Fig. 4b). By 2017, and following mass bleaching, hard coral cover was no longer significantly spatially structured around the island and was indiscernible from a random distribution at all scales (Fig. 4a).

Like hard coral, CCA showed consistent patterns of spatial structure in 2008 and following minor bleaching in 2010 and was significantly clustered up to 0.9 and 1.0 km scales (Fig. 5a, Supplemental Fig. A3). By the onset of mass bleaching in 2015, the scale at which CCA cover was clustered dropped to 0.5 km and the overall degree of clustering declined (Fig. 5a). Similarly, the degree of spatial clustering of turf algae declined over time through to the onset of mass bleaching (Fig. 5b, Supplemental Fig. A4). Notably, following mass bleaching, both CCA and turf algae became more spatially clustered at larger scales (200-700 m) (Fig. 5a and 5b). In contrast, the spatial structure of fleshy macroalgae changed the least over time and was significantly clustered up to scales of ~0.5 km across all survey years, before and after the bleaching events (Fig. 5c, Supplemental Fig. A5).

The predictability of benthic communities following bleaching

The ability of island geo-region, sub-surface seawater temperature and surface wave power to explain intra-island spatial variation in coral reef benthic communities decreased

between the beginning (2008) and end of the timeseries (2017). In 2008 prior to bleaching, cross-validated percentage deviance explained equalled 55.7% and 53.0% for CCA and turf algae cover, respectively. By 2017 and following the two bleaching events, it equalled 14.4% and 8.0% for CCA and turf algae, respectively (see Supplemental Table A9 for detailed model summary outputs and relative influence of the predictor variables by survey year and see Supplemental Fig. A6-A7 for the response-predictor relationships by survey year). This loss of predictability in turf algae and CCA cover around the island was mirrored when considering all benthic variables simultaneously. In 2008, 24.9% of the benthic community variation across grid cells was explained, but this dropped to 15.3% by 2017 (see Supplemental Table A10).

Discussion

Using a remote coral reef free from local human impacts, we show that repeat coral bleaching can dramatically reduce the cover of calcifying benthic organisms, homogenise benthic communities, and disrupt their natural patterns of spatial organisation across the seascape. This results in a breakdown of the relationship between spatial patterns in the cover of benthic organisms and concurrent gradients in natural environmental drivers. Subsequently, the drivers no longer provide predictive power over the island's benthic seascape ecology, at least in the short-term or perhaps under frequent bleaching disturbance. Our results suggest that coral bleaching can disrupt the natural spatial properties of coral reefs, detected through expansive sampling that would otherwise be missed by more spatially limited observations.

Bleaching alters benthic community composition at a remote reef

Our study showed that even the most remote and protected coral reefs can be vulnerable to climate change. Despite being labelled as the world's healthiest marine ecosystem in 2012 (Halpern *et al.*, 2012), mean hard coral cover around Jarvis Island dropped from 27.0% to 0.3% following mass coral bleaching. This exceptional amount of coral mortality was due to sustained high temperature stress and a temporary reduction in primary production, caused by reduced coastal upwelling, that otherwise might have provided corals with energetic subsidies (Brainard *et al.*, 2018). Following extensive coral mortality, the benthos became characterised by non-reef-building benthic organisms in comparison with the pre-bleaching baseline, notably fleshy turf algae, the fleshy macroalgae *Lobophora* and *Dictyosphaeria*, the calcified macroalga *Galaxaura*, and cyanobacteria. Turf algal assemblages are highly competitive with corals (Barott *et al.*, 2012), but also provide substrate for other macroalgae to grow and can inhibit coral recovery (Nieder *et al.*, 2019). The fast-growing, mat-forming cyanobacteria can smother and outcompete other benthic organisms following acute disturbance, while their low palatability implies a lack of control by herbivory (Ford *et al.*, 2021b). Benthic dominance by fleshy organisms is typically characteristic of reefs chronically impacted by local human impacts (Smith *et al.*, 2016) but can also result from acute heat stress and mass bleaching (Graham *et al.*, 2015) even in the absence of local human impacts (Gilmour *et al.*, 2013).

Mass bleaching at Jarvis also resulted in altered hard coral assemblages. Prior to mass bleaching and even following minor bleaching, coral assemblages were dominated by *Montipora*, with this single genus averaging 20.6% of the benthos around Jarvis between 2008-2015. *Montipora* subsequently suffered extreme (near 100%) mortality following mass bleaching, confirming previous observations at Jarvis over more spatially limited extents (Vargas-Ángel *et al.*, 2019). Overall, our results and those of (Vargas-Ángel *et al.*, 2019) indicate that such high dominance by a single susceptible coral genus leaves a reef vulnerable

to spatially extensive coral mortality following severe heat stress. Following mass bleaching, the surviving corals were from the genera *Porites, Favia, Favites* and *Pocillopora.* These corals likely represented survivors from the mass bleaching event since poritid and faviid corals are stress-tolerant genera (Donner, Kirata and Vieux, 2010; Kayal *et al.*, 2015) and survived mass bleaching in the Persian Gulf and East China Sea (Woesik *et al.*, 2011; Bento *et al.*, 2016). Different species of *Pocillopora* can vary in survival from bleaching events, but the genus as a whole shows resilience (Burgess *et al.*, 2021). This altered hard coral composition at Jarvis could persist and cause the emergence of increasingly reported novel hard coral assemblages following mass bleaching (Hughes *et al.*, 2018b; Raj *et al.*, 2021).

Bleaching homogenises coral reef benthic communities

Ecological communities can become more biotically heterogenous with increased species diversity following various types of disturbances (Odum, 1985; Gerwing *et al.*, 2018). Here we found that benthic communities exhibited biotic homogenisation and became more spatially similar around Jarvis following both minor and mass bleaching disturbance. Similarly, models predicted homogenisation of coral communities across the remote Chagos Archipelago in the Indian Ocean under realistic climate change disturbance scenarios (Riegl, Sheppard and Purkis, 2012). At Jarvis, the biotic homogenisation of benthic communities appears to be the result of low coral survivorship following mass bleaching and a spatially consistent increase in turf algae cover leading to a more homogenous seascape. Jarvis' abundant herbivorous fish populations (Williams et al., 2015b) could have maintained the spatial dominance of early successional turf algae through top-down control of fleshy macroalgae. Jarvis' remote location and paucity of larval supply (Maragos *et al.*, 2008) could have inhibited coral recovery despite abundant CCA following mass bleaching that facilitates coral recruitment (Price, 2010). Our data do not span a sufficient post-disturbance period to

know whether Jarvis' benthic community will remain in a homogenised state. However by 2018, less spatially expansive surveys showed the post-bleaching dominance by fleshy macroalgae and turf algae was only temporary; these were rapidly outcompeted by calcifying CCA and macroalgae from the genus *Halimeda* (Huntington *et al.*, 2022). It is therefore likely that the spatially expansive homogenisation of the benthic communities we document here is a temporary phenomenon at this remote reef.

Bleaching events disrupt the spatial properties of benthic communities across scales

Increased community diversity and spatial heterogeneity following disturbance, even following severe disturbance, has generally been the rule rather than the exception in landscape ecology studies (Turner, 2010). However there are some exceptions, like severe wind disturbance leading to decreased spatial clustering of trees across North American forest landscapes (Peterson, 2020). Here we find the same phenomenon in tropical marine benthic communities – recurrent bleaching resulted in the loss of significant spatial structure in hard coral cover around the island. The spatial clustering evident prior to mass bleaching broke down, resulting in a spatially random distribution of surviving coral cover across all scales examined.

The reduced degree of hard coral cover spatial clustering was already evident during the onset of mass bleaching in 2015 and before any dramatic wholesale loss in island-mean coral cover at Jarvis. This may reflect residual impacts of the more minor marine heatwave that occurred five years earlier (Vargas-Ángel *et al.*, 2011). Reductions in hard coral spatial clustering may therefore offer an indicator of the ecosystem already becoming degraded. Decreased numbers of large patches of vegetation and increased spatial homogeneity in habitat across landscapes are considered indicative of degraded systems within grasslands (Meyers, Dekeyser and Norland, 2014), intertidal mudflats (Weerman *et al.*, 2012) and arid

ecosystems (Kefi *et al.*, 2007). A more random distribution of hard coral cover following mass bleaching on coral reefs could have ecosystem recovery implications, since less aggregated coral communities recover to pre-disturbance states less effectively under modelled scenarios (Brito-Millán *et al.*, 2019).

Like hard coral, the cover of CCA and turf algae generally became less spatially clustered following bleaching, particularly at smaller (100 m) scales. CCA and turf algae are naturally spatially clustered around Jarvis due to gradients in key environmental drivers that themselves exhibit strong degrees of spatial clustering (Ford *et al.*, 2021a) (Supplemental Fig. A2). The reduction in the degree of spatial clustering and increasingly random distribution of CCA and turf algae following bleaching may reflect their opportunistic colonisation of newly available substrate in areas of localised high coral mortality. In contrast to hard coral cover, however, both CCA and turf algae became more spatially clustered at larger scales (200-700 m) following mass bleaching and this may reflect the occurrence of larger patches with a consistent amount of cover (Supplemental Fig. A3-A4). In contrast to the other benthic groups, fleshy macroalgae around Jarvis remained spatially clustered up to ~500 m scales following both bleaching events, despite an overall island-mean increase in cover following mass bleaching. The persistent spatial clustering of fleshy macroalgae both before and after bleaching disturbance is intriguing and warrants further investigation as to the driving forces behind their stable spatial properties.

Bleaching events disrupt the spatial predictability of coral reef benthic communities

The ability of long-term environmental drivers to effectively predict spatial variations in coral reef ecosystem state appears to be compromised under chronic local human impacts (Ford et al., 2020; Williams et al., 2015a). Here we show this concept extends to acute disturbance by anthropogenic climate change. Following bleaching, benthic organism spatial

distributions around Jarvis became substantially less predictable using concurrent gradients in environmental drivers, despite the intra-island gradients in these environmental variables remaining relatively consistent across survey years (Supplemental Fig. A2). Bleaching-induced coral mortality, and the subsequent succession of newly available substrate, therefore appears capable of disrupting the spatial structure of entire benthic communities across the seascape, meaning their distribution patterns no longer reflect long-term environmental forcing. In tropical rainforests, disturbance intensity predicted forest structure and diversity better than long-term environmental variables (Ding *et al.*, 2012). Similarly, in grassland communities, stochasticity in community succession and loss in predictability by abiotic conditions was found after an extreme climatic event (Kreyling, Jentsch and Beierkuhnlein, 2011). Our findings also align with successional theory, that after large infrequent disturbances and when the recovering area is far from propagule sources, community composition is less predictable, owing to more stochastic processes driving their spatial structure (Turner *et al.*, 1998). The degree to which a disturbance homogenises a community and reduces the predictability of communities is likely linked to the severity of the disturbance. As in terrestrial ecosystems, the loss in the spatial predictability of tropical benthic communities may only be temporary. As Jarvis' benthic community begins to recover (Huntington *et al.*, 2022), niche-based processes may act to structure their spatial distributions (assuming differences among benthic organisms), becoming reflective once again of their surrounding long-term environmental setting (Mežaka *et al.*, 2021).

Conclusion

Here we show that coral bleaching can disrupt the natural spatial properties of benthic communities on a tropical coral reef. Two marine heatwaves over a 9-year period resulted in a minor and severe mass coral bleaching event at one of the world's most remote and

protected reef ecosystems, the latter of which caused extensive coral mortality. Following each bleaching event, benthic communities became more taxonomically homogenous and key reef-building benthic organisms like hard corals lost their natural patterns of spatial clustering and became more randomly distributed across scales. As a result of these disruptions to their natural spatial ecology, benthic communities became less spatially predictable and were no longer reflective of gradients in long-term environmental drivers. Instead, their spatial patterns reflected intense and acute disturbance. Our data provides empirical evidence that global warming-induced marine heatwaves are capable of fundamentally re-structuring the spatial properties of tropical coral reef benthic communities across scales.

Acknowledgements: We thank NOAA's Pacific Islands Fisheries Science Center (PIFSC) Ecosystem Sciences Division and the officers and crews of the NOAA ships Hi'ialakai and Oscar Elton Sette for coordinating and carrying out all towed-diver surveys. We also thank the Reef Systems Lab at Bangor University for collective advice and Amanda Dillon at Aline Design for help with figure formatting. Funding: HVF was supported by an Envision Doctoral Training Programme scholarship funded by the Natural Environment Research Council (NERC) of the UK. Additional funds were provided by The Nature Conservancy (Hawai'i and Palmyra Program). Authors' contributions: HVF and GJW conceived the study; HVF performed all data analyses using methods conceived and developed with GJW and AJD; HVF led the writing of the manuscript with GJW. All other authors reviewed the final text.

References

Anderson, M., Gorley, R.N. and Clarke, R.K. (2008) *PERMANOVA+ for PRIMER: Guide to software and statistical methods*.

Anderson, M.J. (2001) ‘A new method for non-parametric multivariate analysis of variance’, *Austral Ecology*, 26(1), pp. 32–46. Available at: https://doi.org/10.1111/J.1442-9993.2001.01070.PP.X.

Anderson, M.J. (2006) ‘Distance-based tests for homogeneity of multivariate dispersions’, *Biometrics*, 62(1), pp. 245–253. Available at: https://doi.org/10.1111/J.1541-0420.2005.00440.X.

Anderson, M.J., Ellingsen, K.E. and McArdle, B.H. (2006) ‘Multivariate dispersion as a measure of beta diversity’, *Ecology Letters*, 9(6), pp. 683–693. Available at: https://doi.org/10.1111/j.1461-0248.2006.00926.x.

Aston, E.A. *et al.* (2019) ‘Scale-dependent spatial patterns in benthic communities around a tropical island seascape’, *Ecography*, 42(3), pp. 578–590. Available at: https://doi.org/10.1111/ecog.04097.

Ateweberhan, M. and McClanahan, T.R. (2010) ‘Relationship between historical sea-surface temperature variability and climate change-induced coral mortality in the western Indian Ocean’, *Marine Pollution Bulletin*, 60(7), pp. 964–970. Available at: https://doi.org/10.1016/J.MARPOLBUL.2010.03.033.

Barkley, H.C. *et al.* (2018) ‘Repeat bleaching of a central Pacific coral reef over the past six decades (1960–2016)’, *Communications Biology*, 1(1), pp. 1–10. Available at: https://doi.org/10.1038/s42003-018-0183-7.

Barott, K. *et al.* (2012) ‘Natural history of coral−algae competition across a gradient of human activity in the Line Islands’, *Marine Ecology Progress Series*, 460, pp. 1–12. Available at: https://doi.org/10.3354/meps09874.

Beijbom, O. *et al.* (2015) ‘Towards Automated Annotation of Benthic Survey Images: Variability of Human Experts and Operational Modes of Automation’, *PLOS ONE*. Edited by C.A. Chen, 10(7), p. e0130312. Available at: https://doi.org/10.1371/journal.pone.0130312.

Bento, R. *et al.* (2016) 'The implications of recurrent disturbances within the world's hottest coral reef', *Marine Pollution Bulletin*, 105(2), pp. 466–472.

Brainard, R., Acoba, T. and Asher, M.A.M. (2019) 'Coral Reef Ecosystem Monitoring Report for the Pacific Remote Islands Marine National Monument 2000-2017', *Pacific Islands Fisheries Science Center, PIFSC Special Publication*, (SP-19-006.), p. 820 p. Available at: https://doi.org/10.25923/T645-DK90.

Brainard, R.E. *et al.* (2018) '5. Ecological impacts of the 2015/16 El Niño in the central equatorial Pacific', *Bulletin of the American Meteorological Society*, 99(1), pp. S21–S26. Available at: https://doi.org/10.1175/BAMS-D-17-0128.1.

Brainard, R.E. *et al.* (2019) *Chapter 4: Jarvis Island. In: Coral Reef Ecosystem Monitoring Report for the Pacific Remote Islands Marine National Monument 2000–2017*. Available at: https://doi.org/10.25923/T645-DK90.

Breiman, L. *et al.* (1984) *Classification and regression trees*. John Wiley & Sons, Ltd. Available at: https://doi.org/10.1002/cyto.990080516.

Brito-Millán, M. *et al.* (2019) 'Influence of aggregation on benthic coral reef spatio-temporal dynamics', *Royal Society Open Science*, 6(2), p. 181703. Available at: http://dx.doi.org/10.1098/rsos.181703Electronicsupplementarymaterialisavailableonlineathttps://doi.org/10.6084/m9.figshare.c.4387988. (Accessed: 9 April 2019).

Brown, B.E. (1997) 'Coral bleaching: causes and consequences', *Coral Reefs 1997 16:1*, 16(1), pp. S129–S138. Available at: https://doi.org/10.1007/S003380050249.

Brusven, M.A. and Rose, S.T. (1981) ' Influence of Substrate Composition and Suspended Sediment on Insect Predation by the Torrent Sculpin, Cottus rhotheus ', *Canadian Journal of Fisheries and Aquatic Sciences*, 38(11), pp. 1444–1448. Available at: https://doi.org/10.1139/F81-191.

Burgess, S.C. *et al.* (2021) 'Response diversity in corals: hidden differences in bleaching

mortality among cryptic Pocillopora species', *Ecology*, 102(6), p. e03324. Available at: https://doi.org/10.1002/ECY.3324.

Burton, P.J., Jentsch, A. and Walker, L.R. (2020) 'The Ecology of Disturbance Interactions', *BioScience*, 70(10), pp. 854–870. Available at: https://doi.org/10.1093/BIOSCI/BIAA088.

Buston, P.M. and Elith, J. (2011) 'Determinants of reproductive success in dominant pairs of clownfish: a boosted regression tree analysis', *Journal of Animal Ecology*, 80(3), pp. 528–538. Available at: https://doi.org/10.1111/J.1365-2656.2011.01803.X.

Cheal, A.J. *et al.* (2017) 'The threat to coral reefs from more intense cyclones under climate change', *Global Change Biology*, 23(4), pp. 1511–1524. Available at: https://doi.org/10.1111/gcb.13593.

Clarke, K.R. and Gorley, R.N. (2015) *Getting started with PRIMER v7*. Available at: www.primer-e.com (Accessed: 12 March 2023).

Coumou, D. and Rahmstorf, S. (2012) 'A decade of weather extremes', *Nature Climate Change*, 2(7), pp. 491–496. Available at: https://doi.org/10.1038/nclimate1452.

Darling, E.S., McClanahan, T.R. and Côté, I.M. (2013) 'Life histories predict coral community disassembly under multiple stressors', *Global Change Biology*, 19(6), pp. 1930–1940. Available at: https://doi.org/10.1111/gcb.12191.

Dilworth, J. *et al.* (2021) 'Host genotype and stable differences in algal symbiont communities explain patterns of thermal stress response of Montipora capitata following thermal pre-exposure and across multiple bleaching events', *Coral Reefs*, 40(1), pp. 151–163. Available at: https://doi.org/10.1007/S00338-020-02024-3.

Ding, Y. *et al.* (2012) 'Recovery of woody plant diversity in tropical rain forests in southern China after logging and shifting cultivation', *Biological Conservation*, 145(1), pp. 225–233. Available at: https://doi.org/10.1016/j.biocon.2011.11.009.

Donner, S.D., Kirata, T. and Vieux, C. (2010) 'Recovery from the 2004 coral bleaching event

in the Gilbert Islands, Kiribati', *Atoll Research Bulletin*, (587), pp. 1–25. Available at: https://doi.org/10.5479/SI.00775630.587.

Dormann, C.F. *et al.* (2013) 'Collinearity: a review of methods to deal with it and a simulation study evaluating their performance', *Ecography*, 36(1), pp. 27–46. Available at: https://doi.org/10.1111/J.1600-0587.2012.07348.X.

Edmunds, P.J. (2014) 'Landscape-scale variation in coral reef community structure in the United States Virgin Islands', *Marine Ecology Progress Series*, 509, pp. 137–152. Available at: https://doi.org/10.3354/meps10891.

Edwards, C.B. *et al.* (2017) 'Large-area imaging reveals biologically driven non-random spatial patterns of corals at a remote reef', *Coral Reefs*, 36(4), pp. 1291–1305. Available at: https://doi.org/10.1007/s00338-017-1624-3.

Elith, J., Leathwick, J.R. and Hastie, T. (2008) 'A working guide to boosted regression trees', *Journal of Animal Ecology*, 77(4), pp. 802–813. Available at: https://doi.org/10.1111/J.1365-2656.2008.01390.X.

Evans, R.D. *et al.* (2020) 'Early recovery dynamics of turbid coral reefs after recurring bleaching events', *Journal of Environmental Management*, 268, p. 110666. Available at: https://doi.org/10.1016/j.jenvman.2020.110666.

Ford, A. *et al.* (2020) 'Local human impacts disrupt relationships between benthic reef assemblages and environmental predictors', *Frontiers in Marine Science*, 7, p. 794. Available at: https://doi.org/10.3389/FMARS.2020.571115.

Ford, H. V. *et al.* (2021a) 'Spatial scaling properties of coral reef benthic communities', *Ecography*, 44(2), pp. 188–198. Available at: https://doi.org/10.1111/ecog.05331.

Ford, A.K. *et al.* (2021b) 'First insights into the impacts of benthic cyanobacterial mats on fish herbivory functions on a nearshore coral reef', *Scientific Reports*, 11(1), pp. 1–14. Available at: https://doi.org/10.1038/s41598-021-84016-z.

Gerwing, T.G. *et al.* (2018) 'Assessing the relationship between community dispersion and disturbance in a soft-sediment ecosystem', *Marine Ecology*, 39(4), p. e12505. Available at: https://doi.org/10.1111/MAEC.12505.

Gilmour, J.P. *et al.* (2013) 'Recovery of an isolated coral reef system following severe disturbance', 340(6128), pp. 69–71. Available at: https://doi.org/10.1126/science.1232310.

Glynn, P.W. (1983) 'Extensive "Bleaching" and Death of Reef Corals on the Pacific Coast of Panamá', *Environmental Conservation*, 10(2), pp. 149–154. Available at: https://doi.org/10.1017/S0376892900012248.

Gove, J.M. *et al.* (2013) 'Quantifying Climatological Ranges and Anomalies for Pacific Coral Reef Ecosystems', *PLoS ONE*. Edited by C. Fulton, 8(4), p. e61974. Available at: https://doi.org/10.1371/journal.pone.0061974.

Gove, J.M. *et al.* (2015) 'Coral reef benthic regimes exhibit non-linear threshold responses to natural physical drivers', 522, pp. 33–48. Available at: https://doi.org/10.3354/meps11118.

Gove, J.M., Merrifield, M.A. and Brainard, R.E. (2006) 'Temporal variability of current-driven upwelling at Jarvis Island', *Journal of Geophysical Research*, 111(C12), p. C12011. Available at: https://doi.org/10.1029/2005JC003161.

Graham, N.A.J. *et al.* (2015) 'Predicting climate-driven regime shifts versus rebound potential in coral reefs', *Nature*, 518(7537), pp. 94–97. Available at: https://doi.org/10.1038/nature14140.

Halpern, B.S. *et al.* (2012) 'An index to assess the health and benefits of the global ocean', *Nature*, 488(7413), pp. 615–620. Available at: https://doi.org/10.1038/nature11397.

Hautier, Y. *et al.* (2017) 'Local loss and spatial homogenization of plant diversity reduce ecosystem multifunctionality', *Nature Ecology & Evolution 2017 2:1*, 2(1), pp. 50–56. Available at: https://doi.org/10.1038/s41559-017-0395-0.

Hobbs, R.J. and Huennneke, L.F. (1992) 'Disturbance, Diversity and Invasion: Implications

for Conservation', *Conservation Biology*, 6(3), pp. 324–337. Available at: https://doi.org/10.1046/j.1523-1739.1992.06030324.x.

Hughes, T.P. *et al.* (2007) 'Phase Shifts, Herbivory, and the Resilience of Coral Reefs to Climate Change', *Current Biology*, 17(4), pp. 360–365. Available at: https://www.sciencedirect.com/science/article/pii/S0960982207008822 (Accessed: 23 March 2018).

Hughes, T.P., Kerry, J.T., *et al.* (2018) 'Global warming transforms coral reef assemblages', *Nature*, 556(7702), pp. 492–496. Available at: https://doi.org/10.1038/s41586-018-0041-2.

Hughes, T.P., Anderson, K.D., *et al.* (2018) 'Spatial and temporal patterns of mass bleaching of corals in the Anthropocene', *Science*, 359(6371), pp. 80–83. Available at: https://doi.org/10.1126/science.aan8048.

Huntington, B. *et al.* (2022) 'Early successional trajectory of benthic community in an uninhabited reef system three years after mass coral bleaching', *Coral Reefs 2022*, pp. 1–10. Available at: https://doi.org/10.1007/S00338-022-02246-7.

Jouffray, J.B. *et al.* (2019) 'Parsing human and biophysical drivers of coral reef regimes', *Proceedings of the Royal Society B: Biological Sciences*, 286(1896), p. 20182544. Available at: https://doi.org/10.1098/rspb.2018.2544.

Kayal, M. *et al.* (2015) 'Searching for the best bet in life-strategy: A quantitative approach to individual performance and population dynamics in reef-building corals', *Ecological Complexity*, 23, pp. 73–84. Available at: https://doi.org/10.1016/J.ECOCOM.2015.07.003.

Kefi, S. *et al.* (2007) 'Spatial vegetation patterns and imminent desertification in Mediterranean arid ecosystems', *Nature*, 449(7159), pp. 213–217. Available at: https://doi.org/10.1038/NATURE06111.

Kenyon, J.C. *et al.* (2006) 'Towed-Diver Surveys, a Method for Mesoscale Spatial Assessment of Benthic Reef Habitat: A Case Study at Midway Atoll in the Hawaiian

Archipelago', *Coastal Management*, 34(3), pp. 339–349. Available at: https://doi.org/10.1080/08920750600686711.

Kreyling, J., Jentsch, A. and Beierkuhnlein, C. (2011) 'Stochastic trajectories of succession initiated by extreme climatic events', *Ecology Letters*, 14(8), pp. 758–764. Available at: https://doi.org/10.1111/j.1461-0248.2011.01637.x.

Maragos, J. *et al.* (2008) 'US Coral Reefs in the Line and Phoenix Islands, Central Pacific Ocean: History, Geology, Oceanography, and Biology', in *Coral Reefs of the USA*. Dordrecht: Springer Netherlands, pp. 595–641. Available at: https://doi.org/10.1007/978-1-4020-6847-8_15.

McArdle, B.H. and Anderson, M.J. (2001) 'Fitting Multivariate Models to Community Data: A Comment on Distance-Based Redundancy Analysis', *Ecology*, 82(1), p. 290. Available at: https://doi.org/10.2307/2680104.

McKinney, M.L. and Lockwood, J.L. (1999) 'Biotic homogenization: a few winners replacing many losers in the next mass extinction', *Trends in Ecology & Evolution*, 14(11), pp. 450–453. Available at: https://doi.org/10.1016/S0169-5347(99)01679-1.

Meyers, L.M., Dekeyser, E.S. and Norland, J.E. (2014) 'Differences in spatial autocorrelation (SAc), plant species richness and diversity, and plant community composition in grazed and ungrazed grasslands along a moisture gradient, North Dakota, USA', *Applied Vegetation Science*. Edited by P. Adler, 17(1), pp. 53–62. Available at: https://doi.org/10.1111/avsc.12040.

Mežaka, A. *et al.* (2021) 'Life on a leaf: The development of spatial structure in epiphyll communities', *Journal of Ecology*, 00, pp. 1–12. Available at: https://doi.org/10.1111/1365-2745.13824.

Moran, P.A.P. (1950) 'Notes on Continuous Stochastic Phenomena', *Biometrika*, 37(1/2), p. 17. Available at: https://doi.org/10.2307/2332142.

Nieder, C. *et al.* (2019) 'Filamentous calcareous alga provides substrate for coral-competitive macroalgae in the degraded lagoon of Dongsha Atoll, Taiwan', *PLOS ONE*, 14(5), p. e0200864. Available at: https://doi.org/10.1371/JOURNAL.PONE.0200864.

NOAA Coral Reef Watch (2000) *NOAA Coral Reef Watch Operational 50-km Satellite Coral Bleaching Degree Heating Weeks Product, Silver Spring, Maryland, USA: NOAA Coral Reef Watch*. Available at: http://coralreefwatch.noaa.gov/satellite/hdf/index.html (Accessed: 13 May 2022).

Odum, E.P. (1985) 'Trends Expected in Stressed Ecosystems', *BioScience*, 35(7), pp. 419–422. Available at: https://doi.org/10.2307/1310021.

Oksanen, J. *et al.* (2019) 'Vegan: Ordination methods, diversity analysis and other functions for community and vegetation ecologists.', *Cran R* [Preprint]. R Package Version. Available at: http://apps.worldagroforestry.org/publication/vegan-community-ecology-package-ordination-methods-diversity-analysis-and-other (Accessed: 17 January 2022).

Olden, J.D. *et al.* (2004) 'Ecological and evolutionary consequences of biotic homogenization', *Trends in Ecology & Evolution*, 19(1), pp. 18–24. Available at: https://doi.org/10.1016/J.TREE.2003.09.010.

Pedersen, N.E. *et al.* (2019) 'The influence of habitat and adults on the spatial distribution of juvenile corals', *Ecography*, 42(10), pp. 1703–1713. Available at: https://doi.org/10.1111/ecog.04520.

Peterson, C.J. (2020) 'Change in Tree Spatial Pattern After Severe Wind Disturbance in Four North American Northern Hardwood and Sub-Boreal Forests', *Frontiers in Forests and Global Change*, 3, p. 57. Available at: https://doi.org/10.3389/FFGC.2020.00057/BIBTEX.

Pickett, S.T.A. and White, P.S. (1985) *The ecology of natural disturbance and patch dynamics, The Ecology of Natural Disturbance and Patch Dynamics*. Academic Press. Available at: https://doi.org/10.2307/2403105.

Plotkin, J.B. *et al.* (2000) 'Species-area Curves, Spatial Aggregation, and Habitat Specialization in Tropical Forests', *Journal of Theoretical Biology*, 207(1), pp. 81–99. Available at: https://doi.org/10.1006/JTBI.2000.2158.

Price, N. (2010) 'Habitat selection, facilitation, and biotic settlement cues affect distribution and performance of coral recruits in French Polynesia', *Oecologia*, 163(3), pp. 747–758. Available at: https://doi.org/10.1007/s00442-010-1578-4.

R Core Team (2020) *R: A laguage and environment for statistical computing*, *R Foundation for Statistical Computing*. Vienna, Austria. Available at: https://www.r-project.org/.

Raj, K.D. *et al.* (2021) 'Coral reef resilience differs among islands within the Gulf of Mannar, southeast India, following successive coral bleaching events', *Coral Reefs*, 40(4), pp. 1029–1044. Available at: https://doi.org/10.1007/s00338-021-02102-0.

Réjou-Méchain, M. *et al.* (2011) 'Spatial aggregation of tropical trees at multiple spatial scales', *Journal of Ecology*, 99(6), pp. 1373–1381. Available at: https://doi.org/10.1111/j.1365-2745.2011.01873.x.

Richardson, L.E. *et al.* (2018) 'Mass coral bleaching causes biotic homogenization of reef fish assemblages', *Global Change Biology*, 24(7), pp. 3117–3129. Available at: https://doi.org/10.1111/gcb.14119.

Riegl, B.M., Sheppard, C.R.C. and Purkis, S.J. (2012) 'Human impact on atolls leads to coral loss and community homogenisation: A modeling study', *PLoS ONE*. Edited by C.R. Voolstra, 7(6), p. e36921. Available at: https://doi.org/10.1371/journal.pone.0036921.

Rigdeway (2015) 'gbm: Generalized Boosted Regression Models', p. 34. Available at: http://cran.r-project.org/web/packages/gbm/index.html%5Cnhttp://code.google.com/p/gradientboostedmode (Accessed: 27 July 2021).

Robinson, J.P.W., Wilson, S.K. and Graham, N.A.J. (2019) 'Abiotic and biotic controls on

coral recovery 16 years after mass bleaching', *Coral Reefs*, 38(6), pp. 1255–1265. Available at: https://doi.org/10.1007/s00338-019-01831-7.

Safaie, A. *et al.* (2018) 'High frequency temperature variability reduces the risk of coral bleaching', *Nature Communications 2018 9:1*, 9(1), pp. 1–12. Available at: https://doi.org/10.1038/s41467-018-04074-2.

Salazar, G. (2020) 'EcolUtils: Utilities for community ecology analysis'. Available at: https://github.com/GuillemSalazar/EcolUtils.

Sheppard, C.R.C., Harris, A. and Sheppard, A.L.S. (2008) 'Archipelago-wide coral recovery patterns since 1998 in the Chagos Archipelago, central Indian Ocean', *Marine Ecology Progress Series*, 362, pp. 109–117. Available at: https://doi.org/10.3354/MEPS07436.

Skirving, W. *et al.* (2020) 'CoralTemp and the Coral Reef Watch Coral Bleaching Heat Stress Product Suite Version 3.1', *Remote Sensing 2020, Vol. 12, Page 3856*, 12(23), p. 3856. Available at: https://doi.org/10.3390/RS12233856.

Smith, J.E. *et al.* (2016) 'Re-evaluating the health of coral reef communities: Baselines and evidence for human impacts across the central pacific', *Proceedings of the Royal Society B: Biological Sciences*, 283(1822), pp. 1–9. Available at: https://doi.org/10.1098/rspb.2015.1985.

Stein, A., Gerstner, K. and Kreft, H. (2014) 'Environmental heterogeneity as a universal driver of species richness across taxa, biomes and spatial scales', *Ecology Letters*, 17(7), pp. 866–880. Available at: https://doi.org/10.1111/ELE.12277.

Turner, M.G. *et al.* (1998) 'Factors Influencing Succession: Lessons from Large, Infrequent Natural Disturbances', *Ecosystems 1998 1:6*, 1(6), pp. 511–523. Available at: https://doi.org/10.1007/S100219900047.

Turner, M.G. (2010) 'Disturbance and landscape dynamics in a changing world', *Ecology*, 91(10), pp. 2833–2849. Available at: https://doi.org/10.1890/10-0097.1.

Vargas-Ángel, B. *et al.* (2011) ‘Severe, widespread El Niño-associated coral bleaching in the US Phoenix Islands’, *Bulletin of Marine Science*, 87(3), pp. 623–638. Available at: https://doi.org/10.5343/bms.2010.1095.

Vargas-Ángel, B. *et al.* (2019) ‘El Niño-associated catastrophic coral mortality at Jarvis Island, central Equatorial Pacific’, *Coral Reefs*, 38(4), pp. 731–741. Available at: https://doi.org/10.1007/s00338-019-01838-0.

Vellend, M. *et al.* (2007) ‘Homogenization of forest plant communities and weakening of species-environment relationships via agricultural land use’, *Journal of Ecology*, 95(3), pp. 565–573. Available at: https://doi.org/10.1111/j.1365-2745.2007.01233.x.

Wang, S. *et al.* (2021) ‘Biotic homogenization destabilizes ecosystem functioning by decreasing spatial asynchrony’, *Ecology*, 102(6), p. e03332. Available at: https://doi.org/10.1002/ECY.3332.

Weerman, E.J. *et al.* (2012) ‘Changes in diatom patch-size distribution and degradation in a spatially self-organized intertidal mudflat ecosystem’, *Ecology*, 93(3), pp. 608–618. Available at: https://doi.org/10.1890/11-0625.1.

Williams, G.J., Knapp, I.S., *et al.* (2010) ‘Modeling patterns of coral bleaching at a remote Central Pacific atoll’, *Marine Pollution Bulletin*, 60(9), pp. 1467–1476. Available at: https://doi.org/10.1016/j.marpolbul.2010.05.009.

Williams, G.J., Aeby, G.S., *et al.* (2010) ‘Predictive Modeling of Coral Disease Distribution within a Reef System’, *PLOS ONE*, 5(2), p. e9264. Available at: https://doi.org/10.1371/JOURNAL.PONE.0009264.

Williams, G.J. *et al.* (2013) ‘Benthic communities at two remote pacific coral reefs: Effects of reef habitat, depth, and wave energy gradients on spatial patterns’, *PeerJ*, 1, p. e81. Available at: https://doi.org/10.7717/peerj.81.

Williams, G.J. *et al.* (2015) ‘Local human impacts decouple natural biophysical relationships

on Pacific coral reefs', *Ecography*, 38(8), pp. 751–761. Available at: https://doi.org/10.1111/ecog.01353.

Williams, G.J. *et al.* (2019) 'Coral reef ecology in the Anthropocene', *Functional Ecology*. Edited by C. Fox, 33(6), pp. 1014–1022. Available at: https://doi.org/10.1111/1365-2435.13290.

Williams, G.J. and Graham, N.A.J. (2019) 'Rethinking coral reef functional futures', *Functional Ecology*, 33(6), pp. 942–947. Available at: https://doi.org/10.1111/1365-2435.13374.

Williams, I.D. *et al.* (2015) 'Human, Oceanographic and Habitat Drivers of Central and Western Pacific Coral Reef Fish Assemblages', *PLOS ONE*, 10(4), p. e0120516. Available at: https://doi.org/10.1371/JOURNAL.PONE.0120516.

Woesik, R. van *et al.* (2011) 'Revisiting the winners and the losers a decade after coral bleaching', *Marine Ecology Progress Series*, 434, pp. 67–76. Available at: https://doi.org/10.3354/MEPS09203.

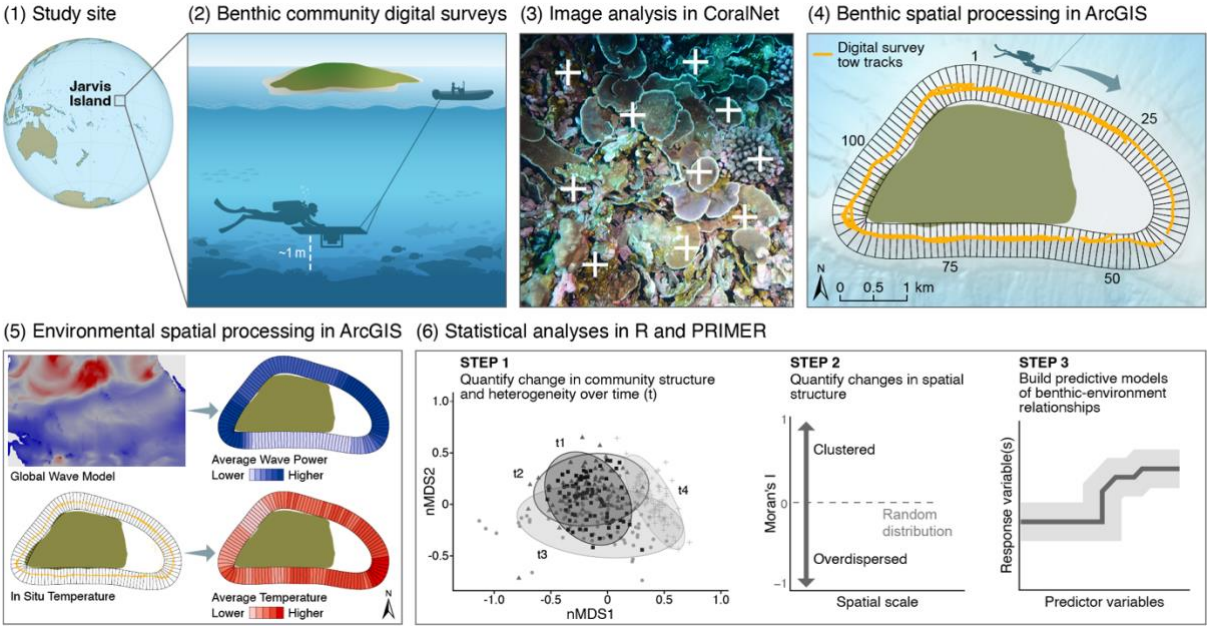

Figure 1. Data collection, processing steps, and analytical pipeline for quantifying changes in coral reef benthic community composition and heterogeneity, spatial structure across scales, and spatial predictability following recurring coral bleaching events at Jarvis Island, central Pacific Ocean.

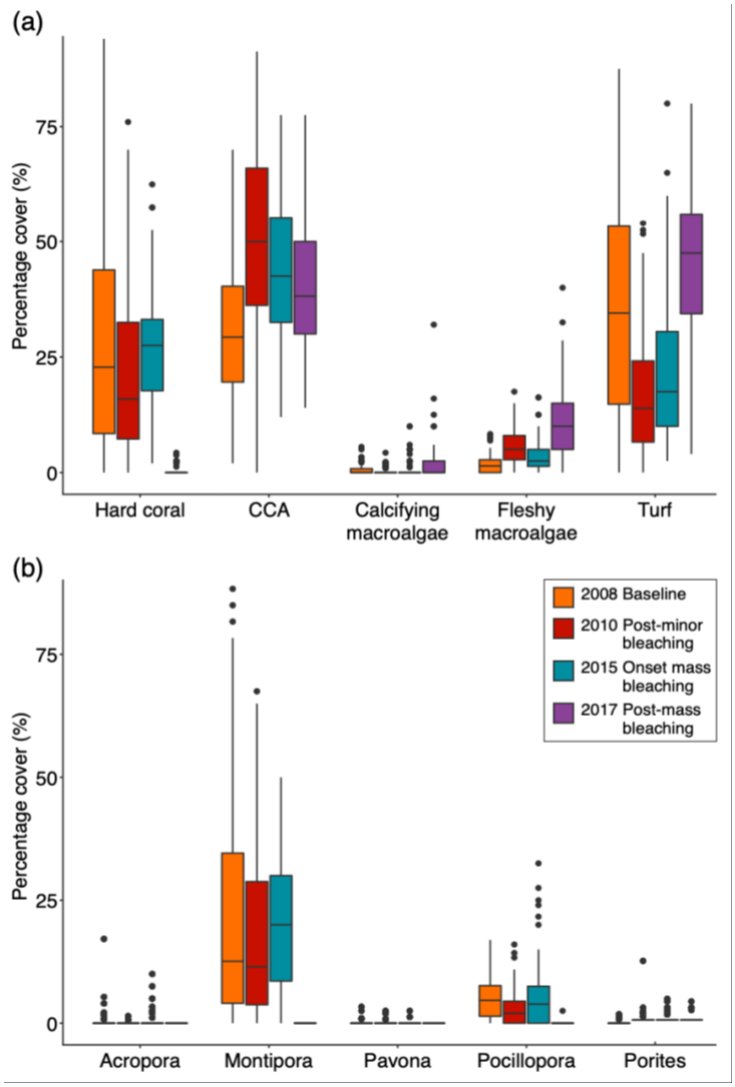

Figure 2. Variation in percentage cover values of the five most dominant benthic groups (a) and the five most dominant hard coral genera (b) before and after two coral bleaching events (one minor, one severe) at ~15 m depth around the ~13 linear km of Jarvis Island's fore-reef habitat at a spatial resolution of 100 m. CCA, crustose coralline algae. Dots here represent outliers and boxes show the interquartile range and their middle lines represent median values.

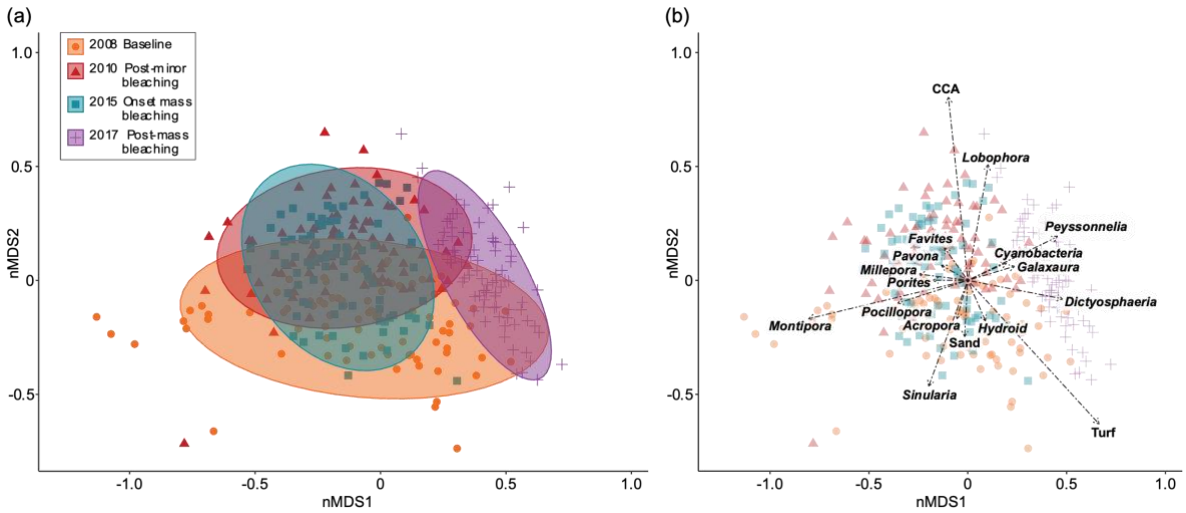

Figure 3. Benthic community change over time around Jarvis Island. a) Differences in community structure grouped and coloured by year with each point at the 100 m grid-cell resolution (n=84 for each year). Shaded circles are the 95% confidence intervals around each year's group centroid (stress = 0.16). Multivariate dispersion (mean distance to centroid) for each year equals 0.2403 (2008), 0.2051 (2010), 0.2031 (2015) and 0.1809 (2017). b) Benthic groups most responsible for driving differences among years. Vector lines in the bi-plot represent correlations (calculated by square root of r^2), with the direction indicating the relationship of each benthic group to the first two ordination axes. The length of each vector line is proportional to the strength of the correlation. Benthic organisms are resolved to genus level for some functional groups including calcifying macroalgae (e.g., *Peyssonnelia*, *Galaxaura*) fleshy macroalgae (e.g., *Lobophora*, *Dictyosphaeria*), hard corals (e.g., *Pavona*, *Favites*, *Pocillopora*, *Montipora*) and soft corals (e.g., *Sinularia*). Others are grouped to a less resolved taxonomic resolution, including fire corals (*Millepora*), Sand, Turf (turf algae) and CCA (crustose coralline algae). See Supplemental Table A2 for a detailed list of the benthic organisms included in the analysis.

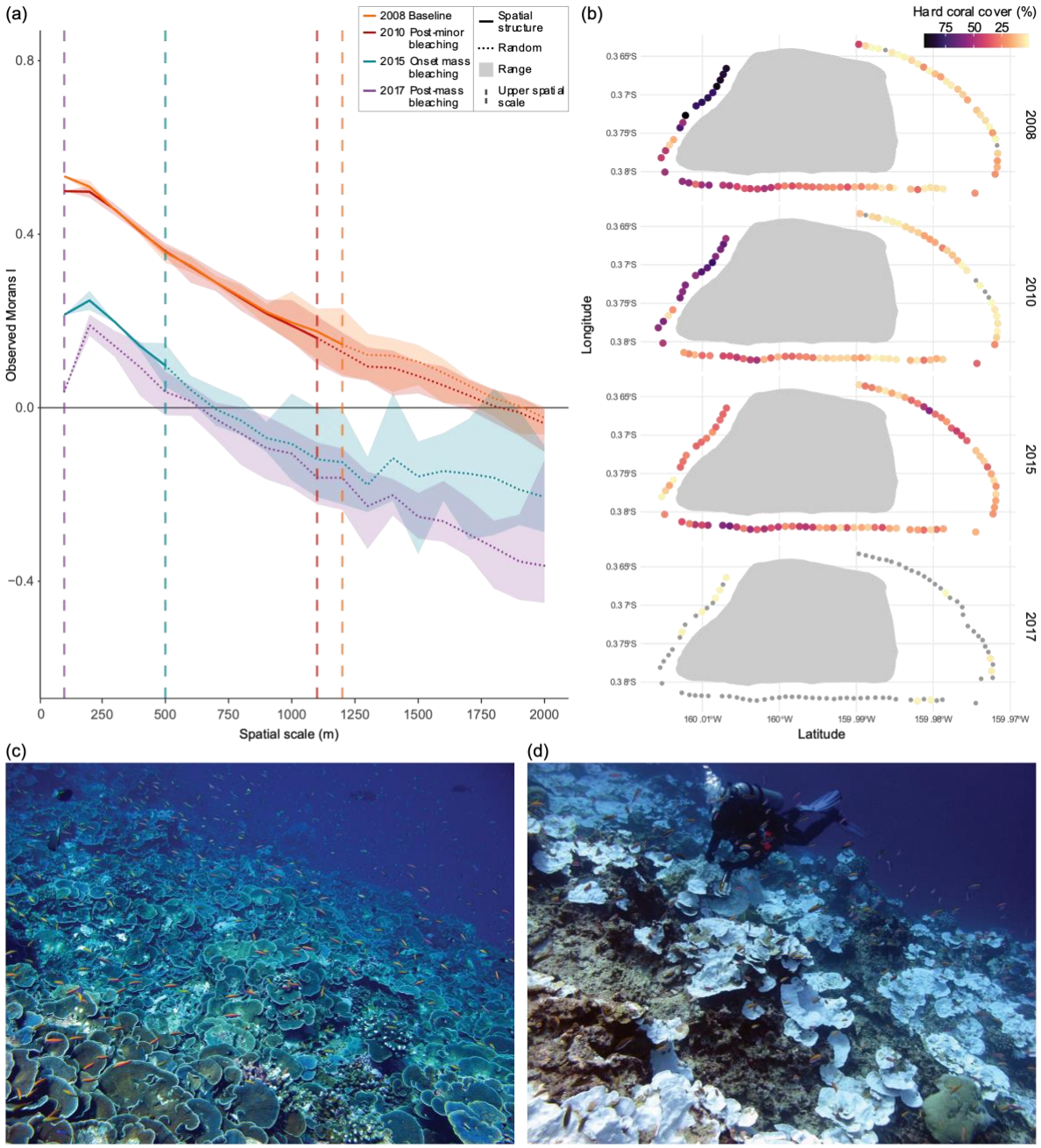

Figure 4. (a) Changes in the spatial structure (solid horizontal lines) of hard coral cover around Jarvis Island over time at increasing 100-m scale increments (starting at 100 m). An Observed Moran's I value away from zero indicates that the spatial pattern of coral cover at that scale is highly organised in space, with positive values indicating a clustered distribution. At each scale we re-computed the range in Moran's I values for all possible 100 m grid cell starting locations iterating in both directions around the circumference of the island (shown as the shaded region around the solid horizontal lines). The vertical dotted lines indicate the upper scale at which there was no longer significant spatial structure in coral cover. Above this scale, the horizontal Moran's I values are dotted to indicate they do not differ from zero (i.e., a random distribution). Despite negative Moran's I values that would indicate overdispersion, none of these values differed from zero and are therefore not interpreted. b) Underlying spatial variation in hard coral cover around the circumference of Jarvis' fore-reef habitat over time (grey shading indicates emergent land). Points represent the average hard coral cover within each 100-m grid

cell (placed at the average latitude and longitude of the geolocated photos within each cell). Grey circles show the location of all photos included for that year where no hard coral cover was present. c) High coral cover along Jarvis' western coast prior to bleaching (image credit: GJW) and d) at the onset of mass bleaching in 2015 (image courtesy of NOAA).

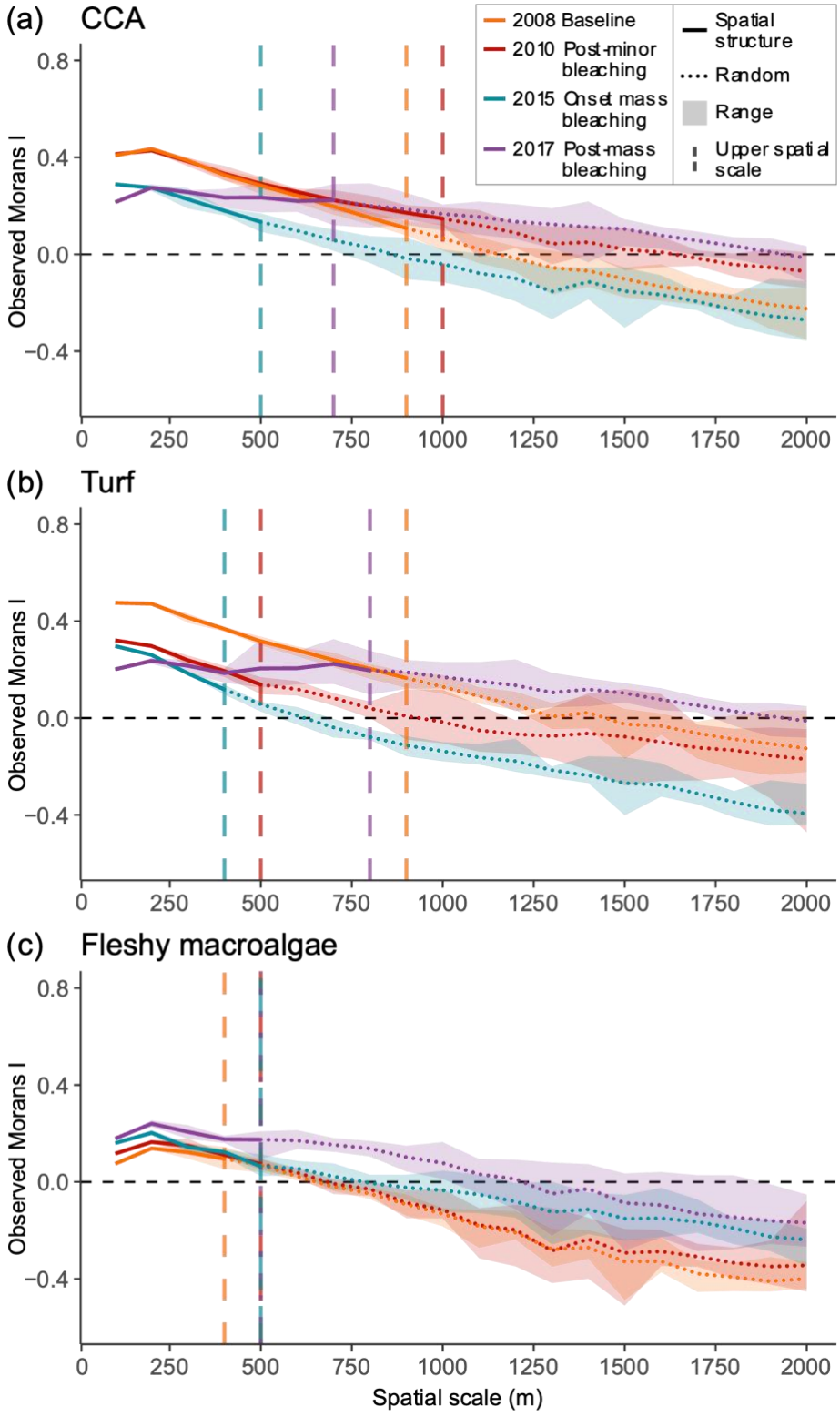

Figure 5. Changes in the spatial structure (solid horizontal lines) of a) crustose coralline algae (CCA), b) turf algae and c) fleshy macroalgae cover around Jarvis Island over time at increasing 100-m scale increments (starting at 100 m). An Observed Moran's I value away from zero indicates that the spatial pattern of coral cover at that scale is highly organised in space, with positive values indicating a clustered distribution. At each scale we re-computed the range in Moran's I values for all possible 100 m grid cell starting locations iterating in both directions around the circumference of the island (shown as the shaded region around the solid horizontal lines). The vertical dotted lines indicate the upper scale at which there was no longer significant spatial structure in cover. Above this scale, the horizontal Moran's I values are dotted to indicate they do not differ from zero (i.e., a random distribution). Despite negative Moran's I values that would indicate overdispersion, none of these values differed from zero and are therefore not interpreted.

Supplementary Material for

Recurring bleaching events disrupt the spatial properties of coral reef benthic communities across scales

Helen V. Ford, Jamison M. Gove, John R. Healey, Andrew J. Davies, Nicholas A. J. Graham, and Gareth J. Williams*

*Corresponding author. Email: g.j.williams@bangor.ac.uk

Table A1. Summary statistics for the number of photos used in the analyses from each survey year.

Year	***2008***	***2010***	***2015***	***2017***
Survey start date	March 26	April 01	April 08	April 02
Survey end date	March 28	April 02	April 08	April 03
Minimum photo per grid cell	4	4	4	4
Maximum photo per grid cell	17	17	10	8
Mean photos per grid cell	9	8	5	5
Total photos per survey	796	699	430	422
Number of grid cells	84	84	84	84

Table A2. Benthic organisms at Jarvis Island identified to genus where possible and categorised into higer-level benthic groups.

Genus (where possible)	Higher-level benthic group
Acropora	Hard coral
Montipora	Hard coral
Porites	Hard coral
Pavona	Hard coral
Stylophora	Hard coral
Leptoseris	Hard coral
Favites	Hard coral
Favia	Hard coral
Fungia	Hard coral
Lobophyllia	Hard coral
Turbinaria	Hard coral
Leptastrea	Hard coral
Pocillopora	Hard coral
Zoanthid	Other invertebrates
Hydroid	Other invertebrates
Millepora	Other invertebrates
Echinoderm	Other invertebrates
Holothuria	Other invertebrates
Sinularia	Soft coral
Clavularia	Soft coral
CCA	CCA
Peyssonnelia	CCA
Turf algae	Turf algae

Halimeda	Calcifying macroalgae
Galaxaura	Calcifying macroalgae
Lobophora	Fleshy macroalgae
Valonia	Fleshy macroalgae
Dictyosphaeria	Fleshy macroalgae
Cyanobacteria	Cyanobacteria
Sand	Sand

Table A3. Higher-level benthic group definitions used during our benthic identification process and their source.

Higher-level benthic groups	**Description**	**Based on source:**
Hard coral	All Scleractinia.	(Veron, 2000)
CCA	Coraline crustose algae. Includes substrate and rubble covered in CCA. Also includes *Peyssonnelia* spp. Which are functionally similar.	(Based on the National Oceanographic and Atmospheric Administration's (NOAA) Pacific Islands Fisheries Science Center (PIFSC) benthic image analysis classification scheme; https://www.fisheries.noaa.gov/inport/item/36380)
Turf algae	Mixture of short often indistinguishable algae. Including the "epilithic algal matrix" and defined as a mixed community of filamentous algae and cyanobacteria generally <2 cm tall, often appearing as fuzzy carpets. Found on hard surfaces, as well as rubble and sand.	(Based on NOAA's PIFSC benthic image analysis classification scheme)
Calcifying macroalgae	Calcifying algae that are visible to the naked eye (typically >2 cm) with evident structure and do not form crusts that adhere to rubble or substrate. Includes *Padina* and *Galaxuara.*	(Littler and Littler, 2003)
Fleshy macroalgae	Fleshy or non-calcifying algae that are visible to the naked eye (typically >2 cm) with evident structure and do not form crusts that adhere to rubble or substrate. Includes *Lobophora* and *Valonia*.	(Littler and Littler, 2003)
Soft coral	All Alcyonacea.	(Fabricius, Alderslade and Australian Institute of Marine Science., 2001)
Other invertebrates	Includes Anemones, Echinoderms, Fire coral, Holothurians and other invertebrates that are not included in other categories.	(Williams *et al.*, 2013)

Sand	Unconsolidated sediment ranging in texture and size from fine to coarse. Assigned to areas clearly distinguished as sand generally >1 cm deep and without anything clearly growing on top.	(Based on NOAA's PIFSC benthic image analysis classification scheme)
Cyanobacteria	Filamentous mat-forming organism.	(Ford *et al.*, 2018)

Table A4. Average distance to centroid of multivariate dispersions over each year with dataset limited to four images per grid cell (as in Fig. A1) and with the data set with a minimum of four images per grid cell but no upper limit (as in Fig. 3). This sensitivity analysis showed little overall variation in the multivariate dispersion between the two approaches.

	Average distance to centroid			
Year	**2008**	**2010**	**2015**	**2017**
Four images per grid cell	0.2477	0.2352	0.2324	0.1804
Minimum of four images per grid cell	0.2388	0.2032	0.2030	0.1791

Table A5-A8. Summary statistics for all benthic organism genera (where possible) at the 100-m grid cell spatial resolution for 2008 (baseline year), 2010 (post-minor bleaching), 2015 (onset mass bleaching) and 2017 (post-mass bleaching). We show the mean and 1 standard error of each group in terms of percentage cover for the entire study extent (island-level, forereef habitat, ~15 m depth) with the higher-level benthic group categories displayed.

A5: 2008			
Genus (where possible)	**Higher-level benthic group**	**Percentage Cover**	
		Mean	**Standard error**
Acropora	Hard coral	0.42	0.22
CCA	CCA	17.89	1.24
Dictyosphaeria	Fleshy macroalgae	0.30	0.09
Echinoderm	Other invertebrates	0.04	0.03
Favia	Hard coral	0.05	0.03
Favites	Hard coral	0.03	0.02
Fungia	Hard coral	0.05	0.03
Galaxaura	Calcifying macroalgae	0.03	0.03
Halimeda	Calcifying macroalgae	0.29	0.08
Holothuria	Other invertebrates	0.01	0.01
Hydnophora	Hard coral	0.01	0.01
Lobophora	Fleshy macroalgae	1.18	0.17
Lobophytum	Soft coral	0.04	0.03

Millepora	Other invertebrates	0.69	0.20
Mollusc	Other invertebrates	0	0
Montipora	Hard coral	22.50	2.58
Pavona	Hard coral	0.10	0.05
Peyssonnelia	CCA	15.94	1.01
Platygyra	Hard coral	0.01	0.01
Pocillopora	Hard coral	5.19	0.50
Porites	Hard coral	0.11	0.04
Sand	Sand	0.26	0.08
Sinularia	Soft coral	2.00	1.24
Stylophora	Hard coral	0.01	0.01
Turf algae	Turf algae	32.81	2.49
Clavularia	Soft coral	0	0
Leptoseris	Hard coral	0	0
Lobophyllia	Hard coral	0	0
Turbinaria	Hard coral	0	0
Valonia	Fleshy macroalgae	0	0
Leptastrea	Hard coral	0	0
Cyanobacteria	Cyanobacteria	0	0
Hydroid	Other invertebrates	0	0

A6: 2010			
Genus (where possible)	**Higher-level benthic group**	**Percentage cover**	
		Mean	**Standard error**
Acropora	Hard coral	0.03	0.02
CCA	CCA	41.96	1.88
Dictyosphaeria	Fleshy macroalgae	0.03	0.02
Echinoderm	Other invertebrates	0.02	0.02
Favia	Hard coral	0.04	0.02
Favites	Hard coral	0.11	0.04
Fungia	Hard coral	0.01	0.01
Galaxaura	Calcifying macroalgae	0	0
Halimeda	Calcifying macroalgae	0.30	0.08
Holothuria	Other invertebrates	0	0
Hydnophora	Hard coral	0.02	0.02
Lobophora	Fleshy macroalgae	5.41	0.44
Lobophytum	Soft coral	0	0
Millepora	Other invertebrates	0.54	0.16
Molluscs	Other invertebrates	0	0
Montipora	Hard coral	19.19	2.09
Pavona	Hard coral	0.14	0.06
Peyssonnelia	CCA	8.49	0.64
Platygyra	Hard coral	0	0

Pocillopora	Hard coral	2.97	0.36
Porites	Hard coral	0.24	0.15
Sand	Sand	0.24	0.17
Sinularia	Soft coral	1.78	1.28
Stylophora	Hard coral	0	0
Turf algae	Turf algae	18.31	1.63
Clavularia	Soft coral	0.01	0.01
Leptoseris	Hard coral	0.01	0.01
Lobophyllia	Hard coral	0.02	0.01
Turbinaria	Hard coral	0.01	0.01
Valonia	Fleshy macroalgae	0.08	0.04
Leptastrea	Hard coral	0	0
Cyanobacteria	Cyanobacteria	0	0
Hydroid	Other invertebrates	0	0

A7: 2015			
Genus (where possible)	**Higher-level benthic group**	**Percentage cover**	
		Mean	**Standard error**
Acropora	Hard coral	0.46	0.18
CCA	CCA	34.59	1.64
Dictyosphaeria	Fleshy macroalgae	0.27	0.08
Echinoderm	Other invertebrates	0	0
Favia	Hard coral	0.05	0.03
Favites	Hard coral	0.07	0.05
Fungia	Hard coral	0.02	0.02
Galaxaura	Calcifying macroalgae	0	0
Halimeda	Calcifying macroalgae	0.83	0.22
Holothuria	Other invertebrates	0	0
Hydnophora	Hard coral	0	0
Lobophora	Fleshy macroalgae	3.54	0.41
Lobophytum	Soft coral	0	0
Millepora	Other invertebrates	0.64	0.22
Molluscs	Other invertebrates	0	0
Montipora	Hard coral	20.23	1.44
Pavona	Hard coral	0.06	0.04
Peyssonnelia	CCA	9.66	0.67
Platygyra	Hard coral	0	0
Pocillopora	Hard coral	5.74	0.75
Porites	Hard coral	0.39	0.10
Sand	Sand	0.36	0.12
Sinularia	Soft coral	0.98	0.77
Stylophora	Hard coral	0	0
Turf algae	Turf algae	22.09	1.85
Clavularia	Soft coral	0	0
Leptoseris	Hard coral	0	0

Lobophyllia	Hard coral	0	0
Turbinaria	Hard coral	0	0
Valonia	Fleshy macroalgae	0	0
Leptastrea	Hard coral	0.02	0.02
Cyanobacteria	Cyanobacteria	0	0
Hydroid	Other invertebrates	0	0

A8: 2017			
Genus (where possible)	**Higher-level benthic group**	**Percentage cover**	
		Mean	**Standard error**
Acropora	Hard coral	0	0
CCA	CCA	22.19	1.31
Dictyosphaeria	Fleshy macroalgae	2.74	0.38
Echinoderm	Other invertebrates	0	0
Favia	Hard coral	0.08	0.05
Favites	Hard coral	0.05	0.04
Fungia	Hard coral	0	0
Galaxaura	Calcifying macroalgae	1.14	0.41
Halimeda	Calcifying macroalgae	0.85	0.19
Holothuria	Other invertebrates	0	0
Hydnophora	Hard coral	0	0
Lobophora	Fleshy macroalgae	8.39	0.96
Lobophytum	Soft coral	0	0
Millepora	Other invertebrates	0	0
Mollusc	Other invertebrates	0	0
Montipora	Hard coral	0	0
Pavona	Hard coral	0	0
Peyssonnelia	CCA	17.36	0.94
Platygyra	Hard coral	0	0
Pocillopora	Hard coral	0.03	0.03
Porites	Hard coral	0.13	0.06
Sand	Sand	0.53	0.25
Sinularia	Soft coral	0.02	0.02
Stylophora	Hard coral	0	0
Turf algae	Turf algae	45.30	1.86
Clavularia	Soft coral	0.05	0.04
Leptoseris	Hard coral	0	0
Lobophyllia	Hard coral	0	0
Turbinaria	Hard coral	0.02	0.02
Valonia	Fleshy macroalgae	0.16	0.08
Leptastrea	Hard coral	0	0
Cyanobacteria	Cyanobacteria	0.85	0.27
Hydroid	Other invertebrates	0.11	0.08

Table A9. Boosted regression tree model performance statistics from predicting the spatial distribution of turf algae and crustose coralline algae (CCA) cover around Jarvis Island based on concurrent gradients in sub-surface seawater temperature and surface wave power. cvPer.Expl (cross-validated percentage deviance explained) is used to assess model performance. Survey years represent the baseline year (2008), post-minor bleaching (2010), onset of mass bleaching (2015), and post-mass bleaching (2017). Per.Expl, Percentage of response variable variation explained; cv, cross-validated.

CCA				
	2008	**2010**	**2015**	**2017**
Tree complexity	3	5	3	3
Learning rate	0.001	0.001	0.0001	0.001
Bag fraction	0.8	0.8	0.8	0.7
Total deviance	228.5	366.4	280.6	201.6
Residual deviance	52.2	72.6	151.9	133.0
Correlation	0.9	0.9	0.7	0.6
Per.Expl	77.1	80.2	45.9	34.0
cvDeviance	101.3	134.0	185.8	172.5
cvCorrelation	0.8	0.8	0.7	0.5
cvPer.Expl	**55.7**	**63.4**	**33.8**	**14.4**
Relative Influence (%):				
Wave power	48.6	9.4	4.3	26.9
Temperature	14.0	70.7	21.7	60.3
Island geo-region	37.4	20.0	74.1	12.9

Turf				
	2008	**2010**	**2015**	**2017**
Tree complexity	4	5	3	5
Learning rate	0.001	0.001	0.001	0.001
Bag fraction	0.5	0.8	0.8	0.5
Total deviance	540.3	221.8	284.3	288.4
Residual deviance	156.7	88.8	81.1	212.9
Correlation	0.8	0.8	0.9	0.5
Per.Expl	71.0	60.0	71.5	26.2
cvDeviance	253.8	154.6	155.1	265.3
cvCorrelation	0.7	0.6	0.7	0.3
cvPer.Expl	**53.0**	**30.3**	**45.5**	**8.0**
Relative Influence (%)				

Wave power	30.0	38.6	23.4	20.7
Temperature	42.2	55.0	47.6	54.2
Island geo-region	27.8	6.4	29.0	20.7

Table A10. Results of permutational distance-based multivariate multiple regression models for each survey year. The multivariate dataset of benthic organisms to genus (30 variables) were modelled against our two environmental variables, sub-surface seawater temperature and surface wave power. Survey years represent the baseline year (2008), post-minor bleaching (2010), onset of mass bleaching (2015), and post-mass bleaching (2017). Total variation explained for each survey year in **bold**.

Year	***Predictor***	***Variation explained (%)***	***Cumulative variation explained (%)***
2008	Temperature	21.2	21.2
	Wave power	3.7	**24.9**
2010	Temperature	25.6	25.6
	Wave power	2.9	**28.5**
2015	Temperature	6.8	6.8
	Wave power	5.0	**11.8**
2017	Temperature	11.9	11.9
	Wave power	3.4	**15.3**

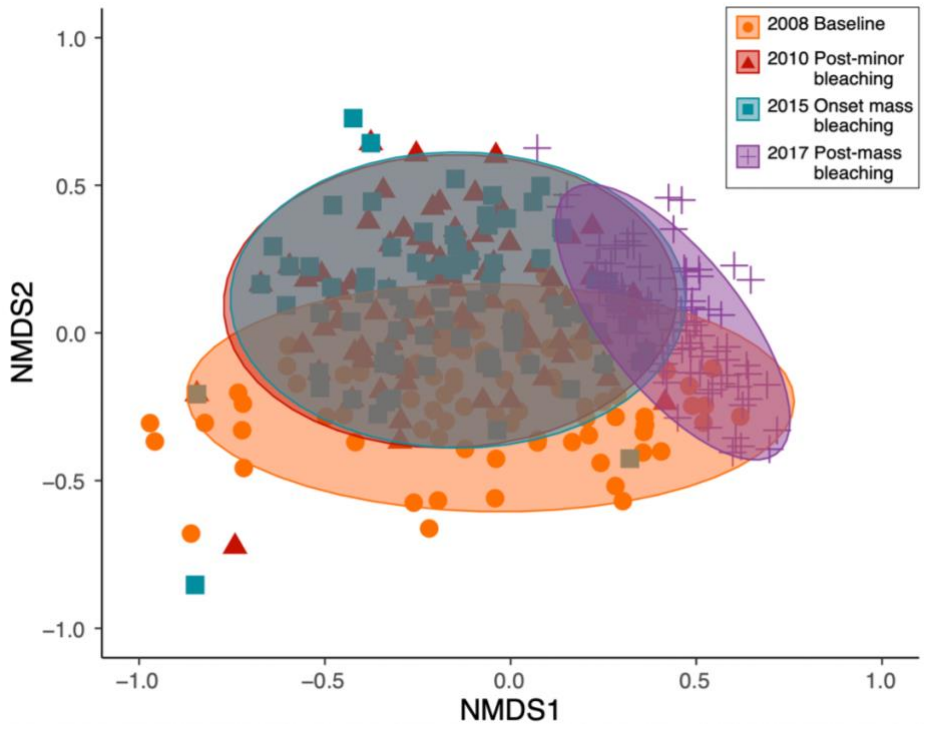

Figure A1. Differences between years in benthic community composition and biotic heterogeneity using only 4 images per grid cell across all survey years. We did this as part of a sensitivity analysis to test for any differences within the multivariate analyses (Fig. 3) that might have resulted from the varying upper limit of images contained within each 100-m grid cell. Here all grid cells used in the analysis contain percentage cover data from only 4 images (obtained by random selection of those present within each grid cell). Shaded circles are the 95% confidence intervals around each year's group centroid (stress = 0.16). Overall, the results revealed the same patterns as the unsubsetted data (where the minimum limit of 4 images per grid cell remained, but no maximum limit was placed on the number of images). Each survey year retained a relative similar degree of multivariate dispersion and 'year' still had a significant effect on benthic community composition (global model = $p<0.05$). Small differences arising from this sensitivity analysis were as follows: 1) the pairwise difference in community composition between the years 2010 and 2015 in the unsubsetted data was no longer significantly different here, and 2) differences in multivariate dispersion between the years 2008 and 2015 in the unsubsetted data was no longer significantly different here. As a result, we chose to retain the original unsubsetted data so as to maximise the accuracy of our percentage cover estimates within any given grid cell.

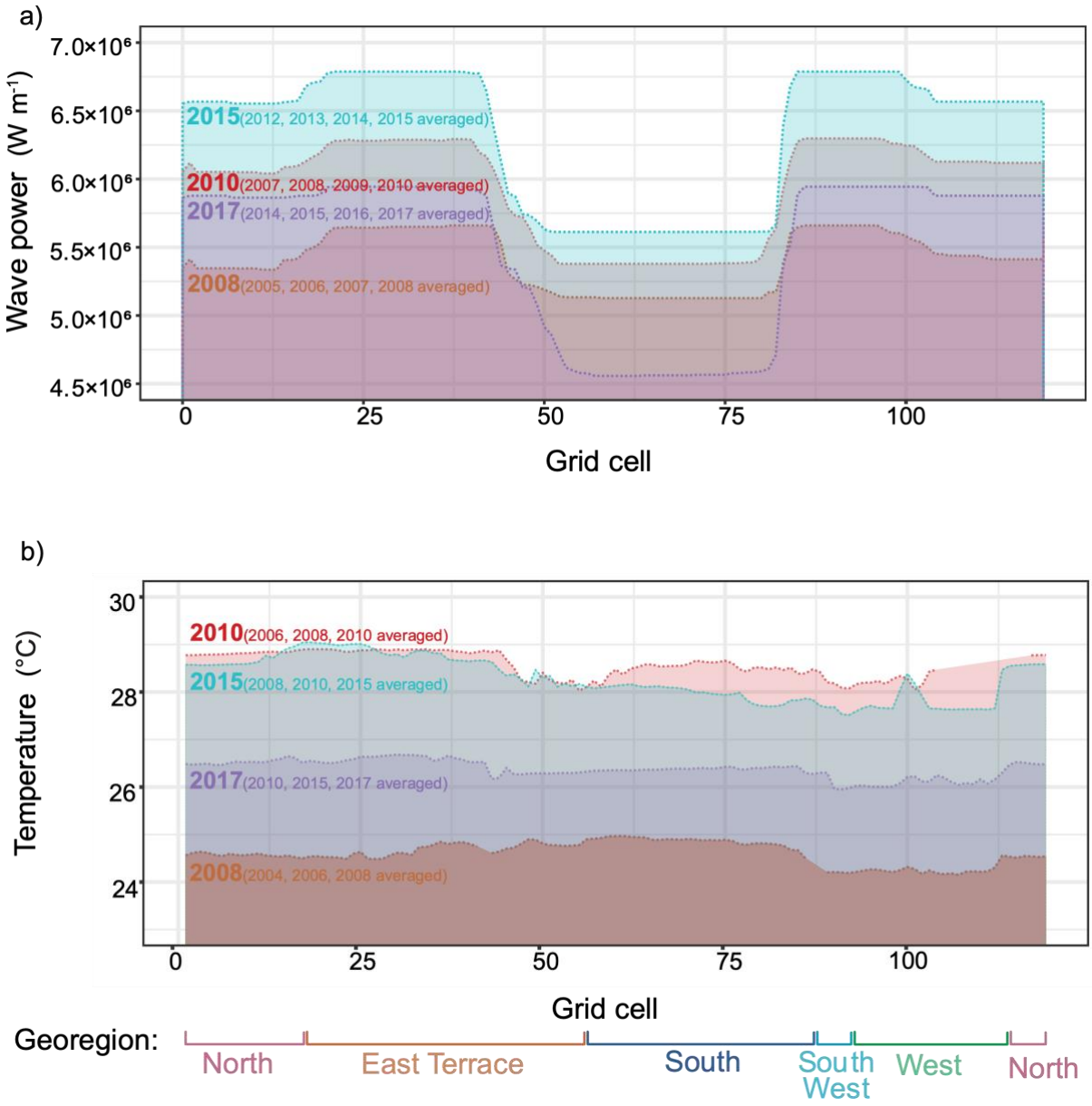

Figure A2. a) Wave power (average of wave anomalies) and b) Temperature (average of sub-surface seawater temperature from years) for each survey year (in bold) around Jarvis Island (by grid cell). Categorical 'geo-region' predictor included in our Boosted Regression Tree models also shown (remained constant across survey years).

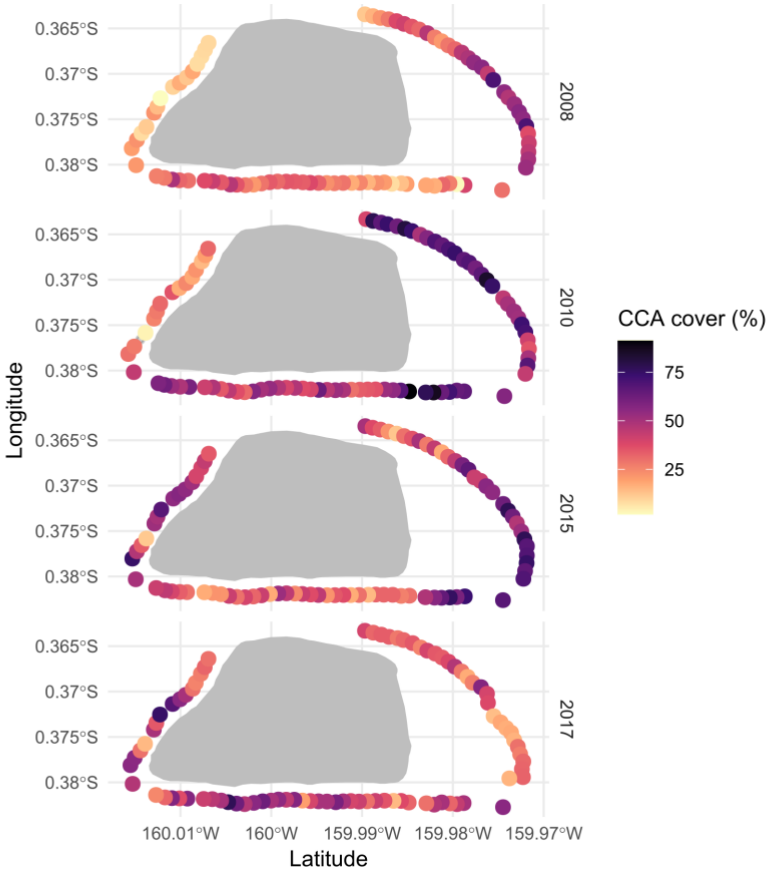

Figure A3. Spatial variation in **crustose coralline algae** (CCA) cover around the circumference of the fore reef habitat of Jarvis Island (central grey shape) over time. Points represent the average CCA cover within each 100-m grid cell (placed at the average latitude and longitude of the geolocated images within each cell). Grey points show the location of all images included for that year where no cover in the respective benthic group was present.

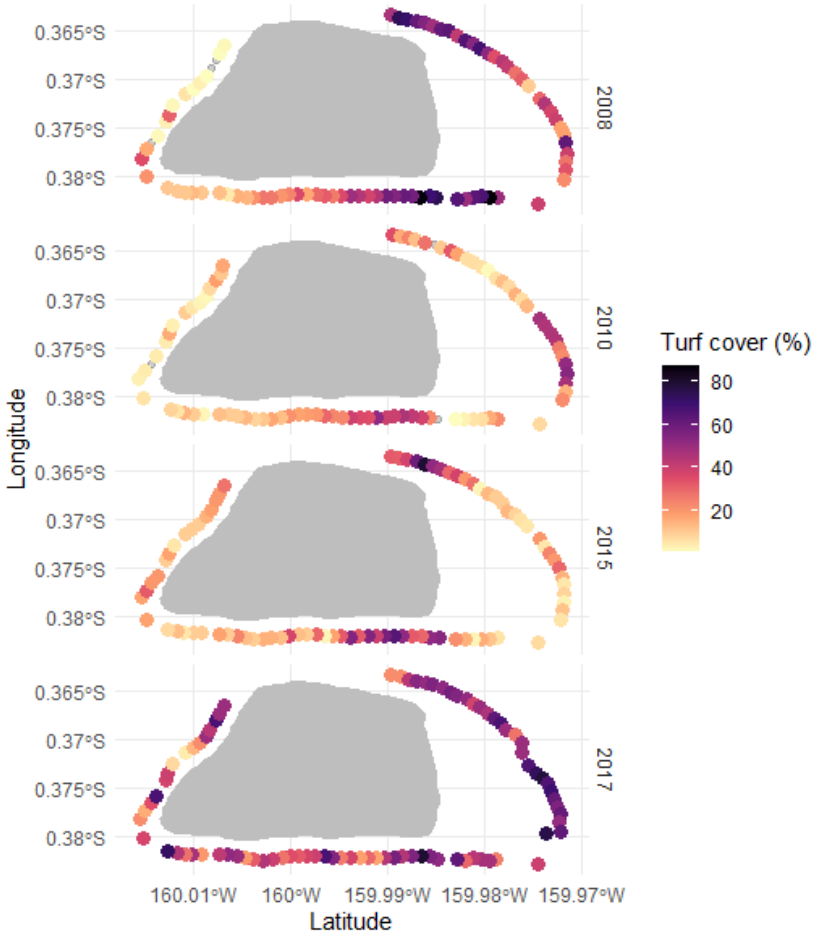

Figure A4. Spatial variation in **turf algae** cover around the circumference of the fore reef habitat of Jarvis Island (central grey shape) over time. Points represent the average turf algae cover within each 100-m grid cell (placed at the average latitude and longitude of the geolocated images within each cell). Grey points show the location of all images included for that year where no cover in the respective benthic group was present.

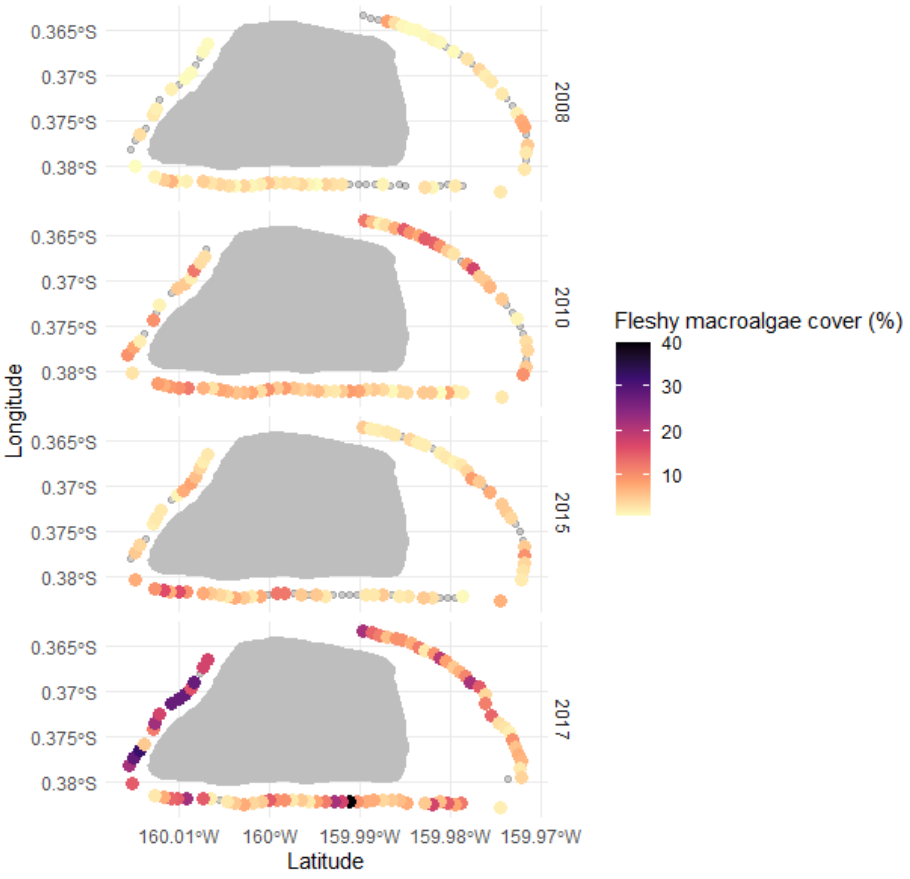

Figure A5. Spatial variation in **fleshy macroalgae** cover around the circumference of the fore reef habitat of Jarvis Island (central grey shape) over time. Points represent the average fleshy macroalgae cover within each 100-m grid cell (placed at the average latitude and longitude of the geolocated images within each cell). Grey points show the location of all images included for that year where no cover in the respective benthic group was present.

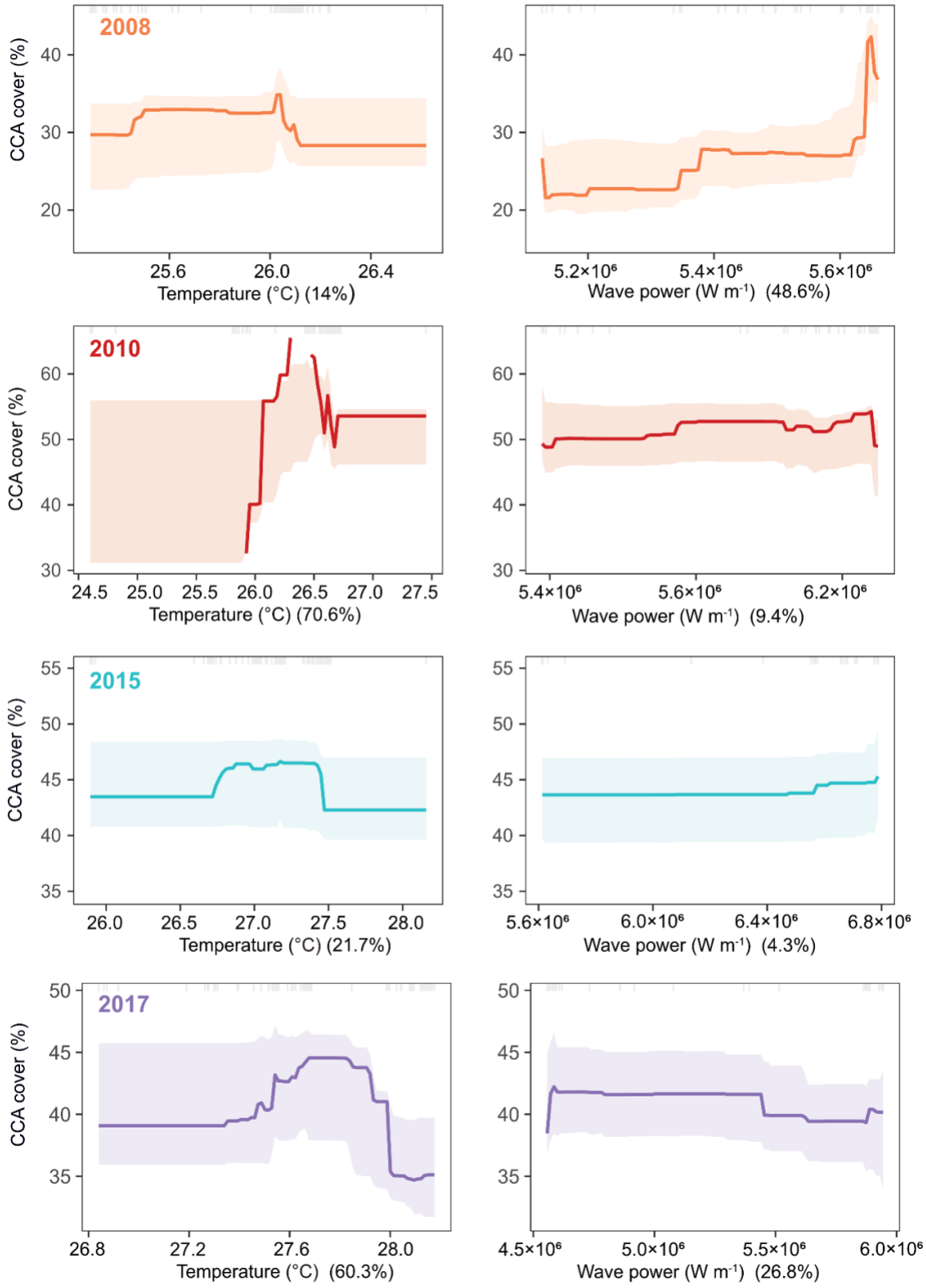

Figure A6. The partial contribution of each predictor variable on the response variable (**percentage cover of crustose coralline algae, CCA**) with temperature shown in the left plot for each year and wave power on the right. The partial contribution for each predictor to the model is shown in brackets. Models for each year are shown from the top 2008 (orange) to 2017 (purple) at the bottom. Bootstrapped 95% confidence intervals (1000 iterations) are shaded either side of the fitted model. Grey tick marks across the top of each plot indicate observed data points.

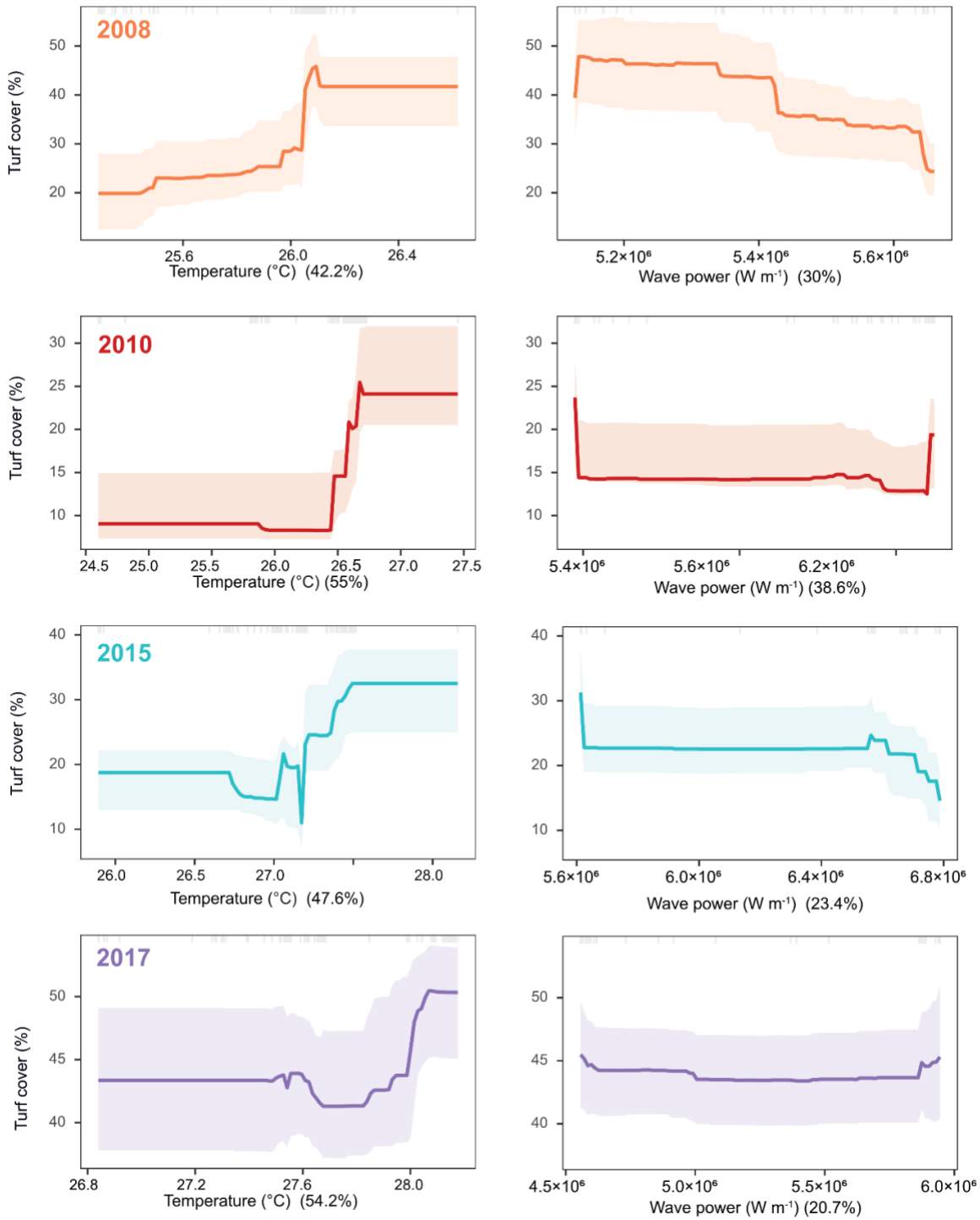

Figure A7. The partial contribution of each predictor variable on the response variable (**percentage cover of turf algae** with temperature shown in the left plot for each year and wave power on the right. The partial contribution for each predictor to the model is shown in brackets. Models for each year are shown from the top 2008 (orange) to 2017 (purple) at the bottom. Bootstrapped 95% confidence intervals (1000 iterations) are shaded either side of the fitted model. Grey tick marks across the top of each plot indicate observed data points.

References

Fabricius, K., Alderslade, P. and Australian Institute of Marine Science. (2001) *Soft corals and sea fans : a comprehensive guide to the tropical shallow water genera of the central-west Pacific, the Indian Ocean and the Red Sea*. Australian Institute of Marine Science

Ford, A.K. *et al.* (2018) 'Reefs under siege-the rise, putative drivers, and consequences of benthic cyanobacterial mats', *Frontiers in Marine Science*, 5(FEB), p. 18. Available at: https://doi.org/10.3389/FMARS.2018.00018/BIBTEX

Littler, D.S. and Littler, M.M. (2003) *South Pacific Reef Plants: A Divers' Guide to the Plant Life of South Pacific Coral Reefs*. California: Offshore Graphics, Incorporated

Veron, J.E.N. (2000) *Corals of the world. Vol 1-3*. Edited by M. Stafford-Smith. Townsville, Australia: Australian Institute of Marine Science

Williams, G.J. *et al.* (2013) 'Benthic communities at two remote pacific coral reefs: Effects of reef habitat, depth, and wave energy gradients on spatial patterns', *PeerJ*, 1, p. e81. Available at: https://doi.org/10.7717/peerj.81